ORGANOMETALLICS

Article

pubs.acs.org/Organometallics

Rare Earth and Main Group Metal Poly(hydrosilyl) Compounds

Nicole L. Lampland,[†] Aradhana Pindwal,[†] KaKing Yan, Arkady Ellern, and Aaron D. Sadow*

Department of Chemistry, Iowa State University, 1605 Gilman Hall, Ames, Iowa 50011, United States

Supporting Information

ABSTRACT: The potassium poly(hydrosilyl) compound $KSi(SiHMe_2)_3$, which contains three β-SiH groups, is synthesized by the reaction of $Si(SiHMe_2)_4$ and KOtBu. A single-crystal X-ray diffraction study reveals chains composed of head-to-tail $KSi(SiHMe_2)_3$ monomers. This potassium poly(hydrosilyl) anion reacts with divalent metal halide salts in THF to form the bis(silyl) compounds $Mg\{Si(SiHMe_2)_3\}_2THF_2$ (**1·THF$_2$**), $Ca\{Si(SiHMe_2)_3\}_2THF_3$ (**2·THF$_3$**), and $Yb\{Si(SiHMe_2)_3\}_2THF_3$ (**3·THF$_3$**). A trivalent yttrium bis(silyl), as part of a KCl-containing polymeric chain, is supported by K←H−Si bridging interactions. The N donors pyridine (**py**) and dimethylaminopyridine (**DMAP**) readily substitute THF, giving tetrahedral magnesium and octahedral calcium silyl compounds. The one-bond silicon−hydrogen coupling constants ($^1J_{SiH}$), infrared stretching frequencies (ν_{SiH}), and solid-state structures of **2·py$_4$** and **3·THF$_3$** indicate classical two center-two electron bonding between the metal center and the silyl ligand, as well as terminal (nonbridging) Si−H bonds within the silyl ligands. The magnesium and calcium compounds readily react with the Lewis acids $PhB(C_6F_5)_2$ and $B(C_6F_5)_3$ to give hydridoborate salts, whereas $\{\kappa^3\text{-To}^M\}_2Yb$ (**5**) (To^M = tris(4,4-dimethyl-2-oxazolinyl)phenyl borate) is formed by reaction of $TlTo^M$ and **3·THF$_3$**.

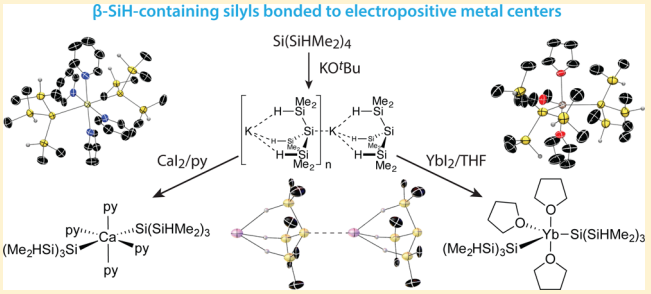

INTRODUCTION

The chemistry of main-group- and rare-earth-metal silyl compounds is underexplored in comparison to silicon chemistry of the transition metals[1] and organometallic chemistry of the main-group metals,[2] both of which are important in wide-ranging synthetic applications. Considering the technological importance of main-group- and rare-earth-silicon compounds, species containing electropositive metal−silicon bonds may have untapped potential applications. For example, $Gd_5Si_2Ge_2$ is used in magnetic refrigeration,[3] and recent catalytic discoveries involving rare-earth compounds and organosilanes include Si−N dehydrocoupling catalyzed by ytterbium or samarium[4] and cerium-catalyzed hydrosilylation of acrylates to give α-silyl esters.[5] These are paralleled by developments in organometallic alkaline-earth-metal-catalyzed processes,[6] highlighted by magnesium- or calcium-catalyzed hydrosilylation of carbonyl compounds.[7]

Isolable homoleptic group 2 and rare earth silyl compounds primarily involve $SiPh_3$ or $Si(SiMe_3)_3$ ligands (Chart 1).[7b,8] Structurally characterized magnesium bis(silyl) compounds also include $Mg(SitBu_3)_2L_2$[1b] and $Mg(SiMe_3)_2L_2$ (L_2 = THF_2, DME, TMEDA).[9] Magnesium and divalent rare-earth metallacyclic polysilyl compounds, including built-in donor groups to control coordination geometry, have also been reported.[10] Such homoleptic compounds are desirable starting materials for new catalysts or materials or as nucleophilic silylating agents, in analogy to the useful chemistry of homoleptic alkyls and amides of early-transition-metal, main-group, and rare-earth species.[11]

The SiH functionality is notably lacking from isolated electropositive rare-earth- and main-group-metal silyl compounds, despite being a critical functionality in hydrosilylations and silane polymerizations mediated by these types of metal sites. For example, alkali-metal silyls are possible intermediates in the Wurtz-type polymerization of chlorosilanes to polysilanes,[12] and SiH-containing silyl anions could lead to other model intermediates including disilenes and silicon-centered radicals. d^0 Transition-metal silyl compounds that contain SiH groups are also intermediates in silane dehydropolymerizations.[13] In these cases, metal silyl intermediates will contain α-SiH, β-SiH, γ-SiH, etc. groups as part of the growing chain [M]−$(SiHR)_n$−X. Silane dehydropolymerizations are proposed to involve σ-bond metathesis steps, and electropositive group 2

Chart 1. Representative Silyl Ligands Supporting Homoleptic Early-Metal Compounds, Tris(dimethylsilyl)methyl and Tetramethyldisilazido Stabilized by Secondary M←H−Si Interactions, and Targeted Tris(dimethylsilyl)silyl Compounds

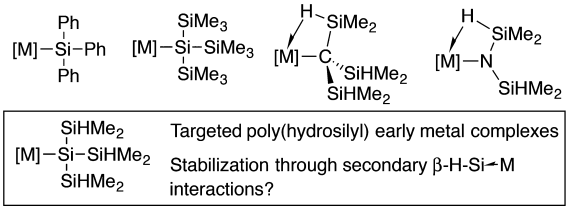

Special Issue: Organometallic Actinide and Lanthanide Chemistry

Received: May 23, 2017

DOI: 10.1021/acs.organomet.7b00383
Organometallics XXXX, XXX, XXX−XXX

and rare-earth-metal silyl compounds might likewise show high reactivity in similar steps. Indeed, related trivalent rare-earth silyl species are implicated in a number of σ-bond metathesis steps.[14] Moreover, β-SiH groups in alkyl and amide ligands form stabilizing secondary interactions with electron-poor metal centers and provide spectroscopic signatures for characterizing structures in homoleptic,[11e,f,l,m,o,15] heteroleptic,[16] and surface-grafted compounds.[11f,o,17] β-SiH groups also provide peripheral sites for reactivity.[18]

These considerations imply that β-SiH groups could stabilize early-metal−silyl ligand bonding through secondary interactions, afford peripheral sites for reactivity, and model steps relevant to catalytic chemistry of organosilanes. We therefore set out to synthesize homoleptic group 1, group 2, and rare-earth-metal compounds containing M−Si(SiHMe$_2$)$_3$ moieties. In fact, LiSi(SiHMe$_2$)$_3$ was first reported by Gilman and coworkers in 1965 as the product of Si(SiHMe$_2$)$_4$ and MeLi.[19] On the basis of our success with potassium tris(dimethylsilyl)methyl (KC(SiHMe$_2$)$_3$) in comparison to its lithium congener,[15a] as well as the versatility of potassium silyl reagents,[1c] we first targeted KSi(SiHMe$_2$)$_3$. Previously, we have used KSi(SiHMe$_2$)$_3$ as a starting point for zinc chemistry.[20]

RESULTS AND DISCUSSION

Synthesis and Characterization of KSi(SiHMe$_2$)$_3$. The potassium silyl species KSi(SiHMe$_2$)$_3$ is the desired reagent to synthesize new metal poly(hydrosilyl) compounds. Its synthesis was briefly reported in a communication,[20a] and a full discussion is given here. The general synthetic scheme involves cleavage of a Si−Si bond of Si(SiHMe$_2$)$_4$ by treatment with KO*t*Bu, and this procedure is based on the preparation of KSi(SiMe$_3$)$_3$ from KO*t*Bu and Si(SiMe$_3$)$_4$.[21] The required precursor Si(SiHMe$_2$)$_4$ is prepared by conversion of Si(SiMe$_3$)$_4$[22] to Si(SiClMe$_2$)$_4$[23] followed by reduction with LiAlH$_4$ (Scheme 1).[24] Although Si(SiMe$_3$)$_4$, AlCl$_3$, and

Scheme 1. Synthesis of Si(SiHMe$_2$)$_4$

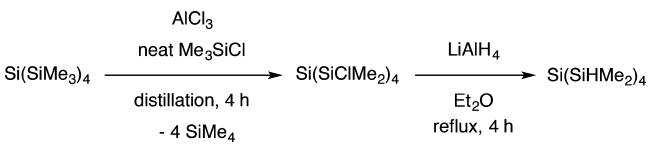

Me$_3$SiCl readily react, a mixture of chlorosilanes is obtained under reflux conditions. Full conversion to Si(SiClMe$_2$)$_4$ is achieved by removing the SiMe$_4$ byproduct as it is formed through careful distillation.[25] In addition, the purity of the AlCl$_3$ is critical for complete conversion to Si(SiClMe$_2$)$_4$, and newly purchased anhydrous AlCl$_3$ also facilitates quantitative conversion. The tetrachlorosilane and LiAlH$_4$ react over 4 h in refluxing diethyl ether to yield Si(SiHMe$_2$)$_4$.[24]

A saturated benzene solution of Si(SiHMe$_2$)$_4$ reacts with KO*t*Bu to form KSi(SiHMe$_2$)$_3$ (eq 1). The product immediately precipitates from the concentrated reaction mixture and is readily isolated in good yield after recrystallization from toluene at −30 °C.

The ^{1}H NMR spectrum of KSi(SiHMe$_2$)$_3$ dissolved in benzene-d_6 contained a doublet at 0.60 ppm assigned to the SiMe$_2$ and a septet at 4.22 ppm assigned to the SiH. This pattern is typical for the series of compounds described in this paper. The chemical shift of the SiMe is apparently influenced

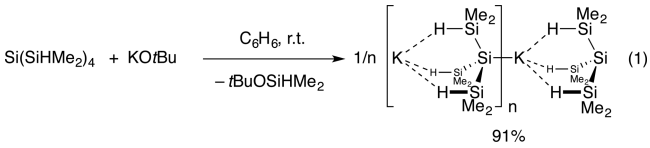

by the element E bonded to the central silicon, E−Si(SiHMe$_2$)$_3$. More electropositive elements result in downfield SiMe signals, whereas less electropositive groups provide compounds with upfield methyl resonances. For example, the ^{1}H NMR chemical shift of the methyl in Si(SiHMe$_2$)$_4$ of 0.31 ppm (E = SiHMe$_2$) is ca. 0.3 ppm upfield of the corresponding resonance in KSi(SiHMe$_2$)$_3$.

The ^{29}Si NMR spectrum of KSi(SiHMe$_2$)$_3$ contained a doublet at −23.8 ppm ($^1J_{SiH}$ = 152 Hz) and a singlet at −202.3 ppm for the SiHMe$_2$ and the internal Si, respectively. These data, as well as the single IR band at 2020 cm^{-1} assigned to the Si−H stretching mode, are intermediate between the values associated with terminal, nonbridging Si−H groups and side-on-coordinated Si−H groups. For example, the ν_{Si-H} band for KSi(SiHMe$_2$)$_3$ appeared at lower energy than for Si(SiHMe$_2$)$_4$ (2093 cm^{-1}), HSi(SiHMe$_2$)$_3$ (2094 cm^{-1}), and HC(SiHMe$_2$)$_3$ (2111 cm^{-1}). In contrast, the IR spectrum of KC(SiHMe$_2$)$_3$ contained two ν_{Si-H} bands at 2108 and 1973 cm^{-1}, with the former likely associated with a linear Si−H−K bridging structure and the latter assigned to a side-on Si−H⇀K interaction (described in greater detail below).[15c]

A single-crystal X-ray diffraction study confirmed the identity of KSi(SiHMe$_2$)$_3$. In the solid state, KSi(SiHMe$_2$)$_3$ forms a chain of alternating potassium cations and Si(SiHMe$_2$)$_3$ anions (Figure 1). KSi(SiHMe$_2$)$_3$ crystallizes in the hexagonal space group $P6_3$, and the K1 and central Si1 are located on a crystallographic 3-fold rotation axis. The central silicon atom of one Si(SiHMe$_2$)$_3$ group is coordinated to the potassium center of the next KSi(SiHMe$_2$)$_3$ monomer, with a K1*−Si1 distance of 3.309(5) Å, to build up the K−[Si(SiHMe$_2$)$_3$−K]$_n$-Si(SiHMe$_2$)$_3$ chains. The K1*−Si1 distance is on the short side for potassium silyl species, which range from 3.3 to 3.6 Å in the Cambridge Structural Database. The next Si(SiHMe$_2$)$_3$ anion in the chain is oriented with three SiHs pointing at the K1 center, and the K1···Si2 distance in these K1−H2s−Si2 structures is 3.872(6) Å. Although the hydrogen atoms on silicon were not located in the Fourier difference map, the tetrahedral Si center and methyl and silicon substituents provide their likely positions between Si and K. In addition, there are three sets of close contacts of silicon methyl groups and the potassium center. These three methyl groups, from three neighboring Si(SiHMe$_2$)$_3$ anions in the surrounding chains, form a trigonal plane around the potassium cation (see the Supporting Information).

The Si2−Si1−Si2# angle is 100.8(2)°, while the K1−Si1−Si2 angle is 117.2(1)°. Thus, the Si1 center is distorted from tetrahedral symmetry with the SiHMe$_2$ groups compressed toward the C_3 axis. Perhaps the three bridging K1−H2s−Si2 interactions pull the SiHMe$_2$ groups to give sharper Si2−Si1−Si2# angles; however, the IR data, namely the ν_{SiH} band, suggest that the Si−H bonds are only weakly perturbed in possible three center-two electron bridges in comparison to two center-two electron SiH bonds in (SiHMe$_2$)$_4$. Alternatively, the K−Me close contacts may affect the overall steric profile of the K1 group (i.e., interchain packing forces). However, the distortion may also be attributed to Bent's rule,[26] because the central Si is bonded to two electropositive elements K and Si.

DOI: 10.1021/acs.organomet.7b00383
Organometallics XXXX, XXX, XXX−XXX

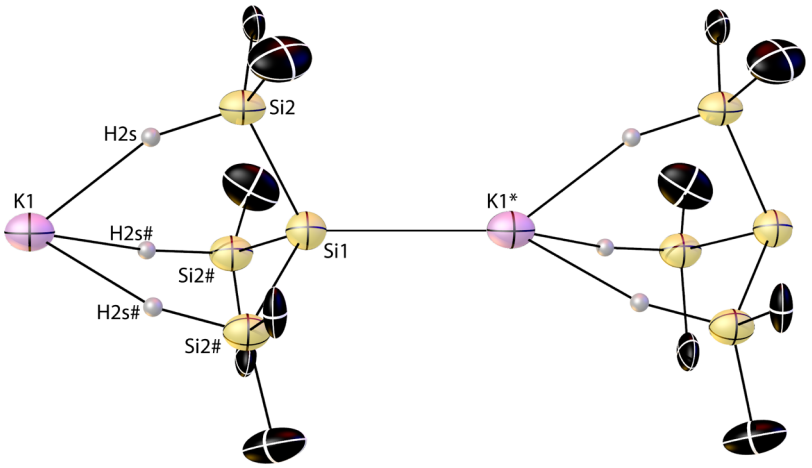

Figure 1. Thermal ellipsoid plot of $KSi(SiHMe_2)_3$ rendered at 35% probability. H2s atoms are placed in calculated positions and are depicted to clarify the geometry. All other H atoms are not illustrated. K1 and Si1 are located on special positions, and the symbols # and * identify positions generated by rotational and translational symmetry, respectively. Selected distances (Å): K1*−Si1, 3.309(7); K1−Si2, 3.872(6); Si1−Si2, 2.297(4). Selected angles (deg): Si2−Si1−Si2#, 100.7(2); K1−Si1−Si2, 117.3(2).

The polarity of the K1−Si1 interaction favors increased s character in that bond, leaving the Si−Si bonds with greater p character and smaller Si2−Si1−Si2# angles.

In contrast to the pseudo-tetrahedral Si1 in $KSi(SiHMe_2)_3$, the potassium alkyl $[(TMEDA)KC(SiHMe_2)_3]_2$ contains a nearly planar carbon center ($\sum$Si−C−Si = 359°).[15c] In addition, two types of nonclassical K−H−Si structures are present in the alkyl dimer: one side-on and two linear bridges in a dimeric structure.[15c] The K−Si distance of the side-on K←H−Si group in that compound is 3.45 Å, whereas the K···Si distances in the end-on K−H−Si groups are 3.983 and 4.096 Å, which are slightly longer than those in $KSi(SiHMe_2)_3$.

There are a number of crystallographically characterized potassium silyl compounds. Most of these contain neutral ligands coordinated to the potassium center, such as 18-crown-6, THF, TMEDA, or an aromatic ring. A few potassium silyl compounds, such as ligand-free $[KSi(SiMe_3)_3]_2$[27] and related $[(18\text{-crown-}6)KSi(SiMe_3)_3]$[28] and $[K(\eta^6\text{-}C_6H_6)_3Si(SiMe_3)_3]$ have been crystallographically characterized. These three compounds contain Si−Si−Si angles of ca. 101.6 ± 0.5°, suggesting that the distorted structure in $KSi(SiHMe_2)_3$ is not a result of packing or the bridging K−H−Si motifs.

Synthesis and Characterization of Divalent Bis(silyl) Compounds. Reactions of $MgBr_2$, CaI_2, or YbI_2 and 2 equiv of $KSi(SiHMe_2)_3$ afford $Mg\{Si(SiHMe_2)_3\}_2THF_2$ (**1·THF$_2$**; eq 2),

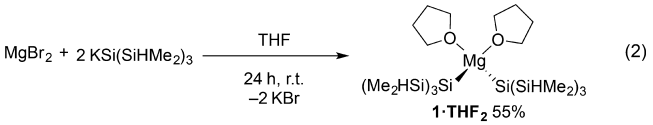

(2)

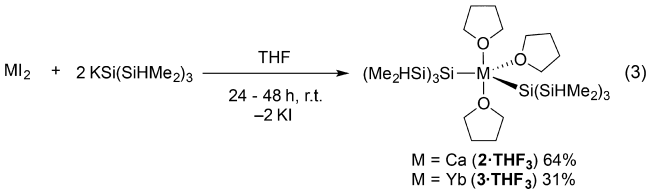

(3)

or $M\{Si(SiHMe_2)_3\}_2THF_3$ (M = Ca, **2·THF$_3$**; M = Yb, **3·THF$_3$**; eq 3). The group 2 silyls are obtained as white pyrophoric solids, while the ytterbium compound crystallizes from pentane as orange needles. We attempted to make low-coordinate, solvent-free Mg and Ca compounds by reacting $MgBr_2$ or CaI_2 and 2 equiv of $KSi(SiHMe_2)_3$ in benzene rather than in THF, but only $KSi(SiHMe_2)_3$ was detected in solution by ^{1}H NMR spectroscopy even after vigorous stirring and heating to 60 °C.

NMR and IR spectral data are given in Tables 1 and 2 for the β-SiH-containing poly(hydrosilyl) complexes. The ^{1}H NMR spectrum of the magnesium compound **1·THF$_2$** contained the expected doublet and septet resonances at 0.56 and 4.58 ppm, respectively, assigned to the SiH and $SiMe_2$. The ^{1}H NMR spectral features of the silyl ligand in **2·THF$_3$** were similar to those of **1·THF$_2$**, while the chemical shifts for **3·THF$_3$** were ca. ∼0.05 ppm further downfield.

The ^{29}Si NMR spectra of **1·THF$_2$**, **2·THF$_3$**, and **3·THF$_3$** (acquired through ^{1}H−^{29}Si HMBC experiments) each contained a signal at ca. −25 ppm and an upfield cross peak that ranged from −170 to −200 ppm. The trend of ^{29}Si NMR chemical shift for the central *Si*$(SiHMe_2)_3$ is as follows: $HSi(SiHMe_2)_3$ > $Si(SiHMe_2)_4$ > **3·THF$_3$** > **1·THF$_2$** > **2·THF$_3$** > $KSi(SiHMe_2)_3$. These signals are upfield with respect to those of the bulky silyl analogues, the values of which are also provided in Table 1 for comparison.[8b] Poor resolution in the indirect dimension limited analysis of ^{171}Yb−^{29}Si coupling.[8f,10,29]

The magnesium disilyl has a higher $^1J_{SiH}$ value in comparison to the calcium and ytterbium congeners, while the potassium silyl is characterized by the lowest $^1J_{SiH}$ value in the series. The chemical shifts and coupling constants in ^{1}H NMR spectra of **2·THF$_3$** or **3·THF$_3$** (toluene-d_8) were essentially invariant from 180 to 298 K, indicating that rotational processes are fast on the ^{1}H NMR time scale. The alkyl analogues $Ca\{C(SiHMe_2)_3\}_2THF_2$ and $Yb\{C(SiHMe_2)_3\}_2THF_2$[15b] were also apparently freely rotating in solution, even at low temperature, although their solid-state structures and IR data supported the presence of secondary interactions. Interestingly, the $^1J_{SiH}$ values for both the silyl compounds (**2·THF$_3$** and **3·THF$_3$**) and alkyl compounds ($Ca\{C(SiHMe_2)_3\}_2THF_2$ and $Yb\{C(SiHMe_2)_3\}_2THF_2$) were all ∼160 Hz. While the similarity between the alkyls and silyls suggested that secondary M←H−Si interactions might be present in the poly(hydrosilyls), that idea is ruled out by other spectroscopic data and crystallo-

DOI: 10.1021/acs.organomet.7b00383
Organometallics XXXX, XXX, XXX−XXX

Table 1. NMR Spectral Data for Main-Group-Metal and Ytterbium Silyl Compounds and Related Silanes (in benzene-d_6)

compound	δ $SiRMe_2$	δ SiH	δ $SiRMe_2$	δ $Si(SiRMe_2)_3$	$^1J_{SiH}$ (Hz)
$KSi(SiHMe_2)_3$[a]	0.56	4.22	−23.8	−202.3	152
$HSi(SiHMe_2)_3$[b]	0.27	4.29	−35.7	−119.2	158, 181
$Si(SiHMe_2)_4$[c]	0.31	4.36	−33.5	−139.9	180
$Mg\{Si(SiHMe_2)_3\}_2THF_2$ (**1·THF$_2$**)	0.56	4.58	−27.5	−182.3	169
$Mg\{Si(SiMe_3)_3\}_2THF_2$[d]	0.46	n.a.	−6.4	−171.9	n.a.
$Mg\{Si(SiHMe_2)_3\}_2py_2$ (**1·py$_2$**)	0.51	4.66	−26.3	−182.2	169
$Mg\{Si(SiHMe_2)_3\}_2DMAP_2$ (**1·DMAP$_2$**)	0.67	4.84	−26.8	−184.3	167
$Ca\{Si(SiHMe_2)_3\}_2THF_3$ (**2·THF$_3$**)	0.57	4.56	−24.6	−194.6	162
$Ca\{Si(SiMe_3)_3\}_2THF_3$[e]	0.50	n.a.	−6.75	−172.3	n.a.
$Ca\{Si(SiHMe_2)_3\}_2py_4$ (**2·py$_4$**)	0.43	4.59	−23.3	−199.3	160
$Ca\{Si(SiHMe_2)_3\}_2DMAP_4$ (**2·DMAP$_4$**)	0.69	4.94	−22.5	−201.5	161
$Yb\{Si(SiHMe_2)_3\}_2THF_3$ (**3·THF$_3$**)	0.61	4.63	−23.6	−168.1	160
$Yb\{Si(SiMe_3)_3\}_2THF_3$[f]	0.48	n.a.	−5.3	−144.8	n.a.

[a]See ref 20a. [b]^{29}Si NMR data were previously reported in ref 30. [c]See ref 24. [d]See ref 8c. [e]See ref 8b. [f]See ref 8f.

Table 2. SiH Stretching Mode for Main-Group-Metal and Ytterbium Silyl Compounds and Related Silanes

compound	ν_{SiH} (KBr, cm^{-1})
$KSi(SiHMe_2)_3$[a]	2020
$HSi(SiHMe_2)_3$	2094 (broad)
$Si(SiHMe_2)_4$	2093
$Mg\{Si(SiHMe_2)_3\}_2THF_2$ (**1·THF$_2$**)	2064
$Mg\{Si(SiHMe_2)_3\}_2py_2$ (**1·py$_2$**)	2067
$Mg\{Si(SiHMe_2)_3\}_2DMAP_2$ (**1·DMAP$_2$**)	2083
$Ca\{Si(SiHMe_2)_3\}_2THF_3$ (**2·THF$_3$**)	2045
$Ca\{Si(SiHMe_2)_3\}_2py_4$ (**2·py$_4$**)	2100
$Ca\{Si(SiHMe_2)_3\}_2DMAP_4$ (**2·DMAP$_4$**)	2036
$Yb\{Si(SiHMe_2)_3\}_2THF_3$ (**3·THF$_3$**)	2045

[a]See ref 20a.

graphic analysis (vide infra). For example, the ν_{SiH} signals in the vibrational spectra appeared as single, high-energy bands at 2064 cm^{-1} for **1·THF$_2$** and 2045 cm^{-1} for **2·THF$_3$** and **3·THF$_3$**. Instead, the trend of $^1J_{SiH}$ follows the trend in Pauling electronegativity values for E in $ESi(SiHMe_2)_3$ ($^1J_{SiH}$ trend, E = H > $SiHMe_2$ > Mg > Ca > Yb > K; Pauling electronegativity, E = H (2.2) > Si (1.9) > Mg (1.31) > Yb (1.26) > Ca (1.0) > K (0.82)).[31] Thus, the variation of $^1J_{SiH}$ values with metal center in $E-Si(SiHMe_2)_3$ compounds is not associated with multicenter interactions but instead follow expectations based on Bent's rule.[26]

The number of coordinated THF molecules was determined from integration of the ^{1}H NMR spectra; however, elemental composition analysis data of these highly air sensitive compounds were consistent with $Mg\{Si(SiHMe_2)_3\}_2THF$ and

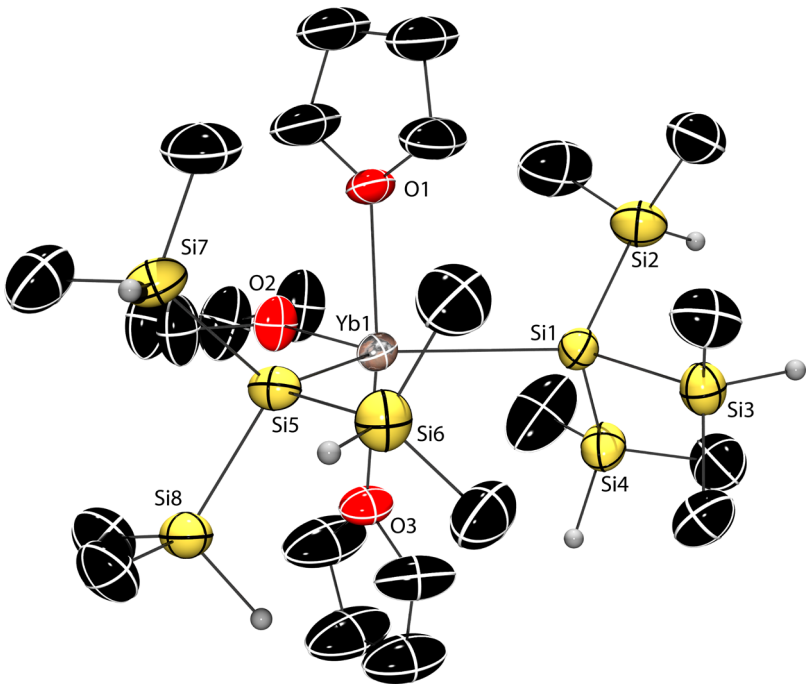

Figure 2. Rendered thermal ellipsoid diagram of $Yb\{Si(SiHMe_2)_3\}_2THF_3$ (**3·THF$_3$**) plotted at 50% probability. H atoms bonded to Si were located objectively in the Fourier difference map and are included in the representation. All other H atoms are not plotted for clarity. The THF ligands are disordered over two positions; only one is illustrated. Significant distances (Å): Yb1−Si1, 3.022(2); Yb1−Si5, 3.011(2), Yb1−O1a, 2.389(4); Yb1−O2a, 2.368(4); Yb1−O3, 2.392(4). Significant angles (deg): Si1−Yb1−Si5, 129.69(6); Si1−Yb1−O1, 90.9(1); Si1−Yb1−O2, 118.1(1); Si1−Yb1−O3, 92.7(1); Si5−Yb1−O1, 94.3(1); Si5−Yb1−O2, 112.2(1); Si5−Yb1−O3, 93.5(1).

DOI: 10.1021/acs.organomet.7b00383
Organometallics XXXX, XXX, XXX−XXX

Scheme 2. Synthetic Routes for the Isolation of 1·py$_2$ and 2·py$_4$

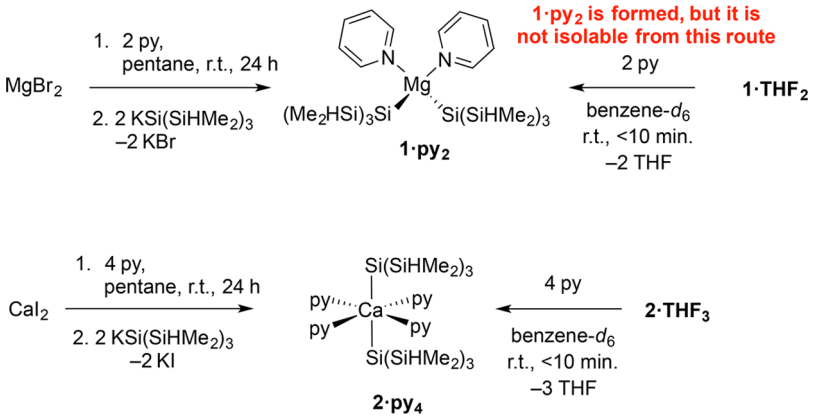

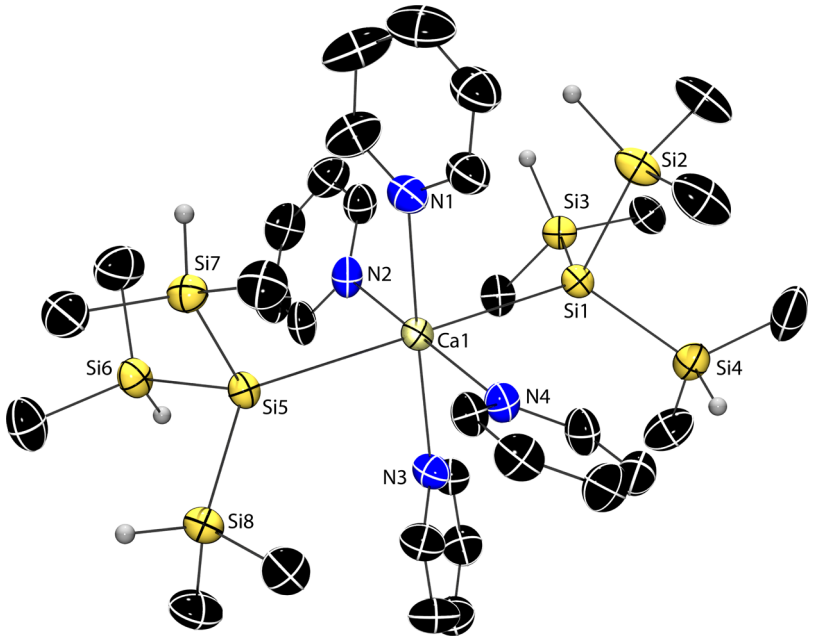

Figure 3. Rendered thermal ellipsoid plot of Ca{Si(SiHMe$_2$)$_3$}$_2$py$_4$ (**2·py$_4$**) depicted at the 50% probability level. Selected distances (Å): Ca1–Si1, 3.147(3); Ca1–Si5, 3.125(3); Ca1–N1, 2.529(7); Ca1–N2, 2.523(7); Ca1–N3, 2.511(7); Ca1–N4, 2.516(6). Selected angles (deg): Si1–Ca1–Si5, 177.8(8); N1–Ca1–N3, 175.0(3); N2–Ca1–N4, 175.5(2); Ca1–Si1–Si2, 108.6(1); Ca1–Si1–Si3, 117.6(1); Ca1–Si1–Si4, 125.7(1); Ca1–Si5–Si6, 113.3(1); Ca1–Si5–Si7, 113.4(1); Ca1–Si5–Si8, 129.2(1); Si2–Si1–Si3, 100.4(1); Si2–Si1–Si4, 101.1(1); Si3–Si1–Si4, 99.6(1); Si6–Si5–Si7, 98.3(1); Si6–Si5–Si8, 98.5(1); Si7–Si5–Si8, 99.2(1).

Ca{Si(SiHMe$_2$)$_3$}$_2$THF$_2$ rather than the higher coordination observed in solution. Despite the apparent lability of THF during combustion analysis, attempts to isolate lower-coordinate compounds by allowing the solids to stand under vacuum provided intractable, unidentified materials. These observations are consistent with the idea that the second and third THF ligands in **1·THF$_2$** and **2·THF$_3$** are labile but required for the persistence of the species in solution and in the solid state.

Additional support for the structure of the compounds is obtained from a single-crystal X-ray diffraction study of **3·THF$_3$**, which crystallizes with a trigonal-bipyramidal geometry (Figure 2). The two Si(SiHMe$_2$)$_3$ groups and one THF occupy the equatorial positions, and the other two THF ligands are axial. The Yb1–Si1 and Yb1–Si5 interatomic distances are 3.022(2) and 3.011(2) Å, respectively. For comparison, the Yb–Si distances in (C$_5$Me$_5$)YbSi(SiMe$_3$)$_3$, Yb{Si(SiMe$_3$)$_3$}$_2$THF$_3$, and Yb(SiPh$_3$)$_2$THF$_4$ are 3.032(2) Å,[29a] 3.064(6) Å,[8f] and 3.158(2) Å,[8a] respectively. The hydrogen atoms bonded to silicon were located objectively in the difference Fourier map. All of the –Si(SiHMe$_2$)$_3$ ligands of **3·THF$_3$** are oriented such that the hydrogen and methyl groups are directed away from the Yb(II) center, in contrast with the dialkyl Yb{C(SiHMe$_2$)$_3$}$_2$THF$_2$, in which the β-SiH groups in the ligand point toward the metal center. The geometry around each Si atom directly bonded to the Yb center is distorted from tetrahedral similarly to the poly(hydrosilyl) group in KSi(SiHMe$_2$)$_3$, with smaller ∠Si–Si–Si (ranging from 97 to 101°) in comparison to ∠Yb–Si–Si (ranging from 111 to 125°). This similarity further suggests that the smaller ∠Si–Si–Si are not the result of the bridging K–H–Si present in KSi(SiHMe$_2$)$_3$.

These compounds are highly air, moisture, and temperature sensitive. Solutions of **1·THF$_2$**, **2·THF$_3$**, and **3·THF$_3$** in benzene-d_6 exposed to air undergo hydrolysis to HSi(SiHMe$_2$)$_3$ essentially instantaneously. In the absence of air, the persistence of magnesium **1·THF$_2$** ($t_{1/2}$ = 48 h, room temperature) in

DOI: 10.1021/acs.organomet.7b00383
Organometallics XXXX, XXX, XXX–XXX

benzene-d_6 is noticeably greater than that of calcium **2·THF$_3$** ($t_{1/2}$ = 12 h, room temperature). Thermolysis of **2·THF$_3$** at 60 °C in benzene-d_6 affords Si(SiHMe$_2$)$_4$ after 12 h as the only observed species in the ^{1}H NMR spectrum, while thermolysis of **1·THF$_2$** at 80 °C for 72 h is required for full conversion to Si(SiHMe$_2$)$_4$. No precipitate was observed in these reactions, and the identities of the metal-containing byproducts have not been established. For comparison, the bulky silyl analogue Ca{Si(SiMe$_3$)$_3$}$_2$THF$_3$ undergoes rapid Si(SiMe$_3$)$_3$ rearrangement to Si(SiMe$_3$)$_4$ upon dissolution in THF,[8b] while the calcium alkyl Ca{C(SiHMe$_2$)$_3$}$_2$THF$_2$ forms HC(SiHMe$_2$)$_3$ after 120 h at 120 °C.

N-Donor-Supported Magnesium and Calcium Disilyl Compounds. We hypothesized that replacing THF might improve crystallinity and the lifetime of the compounds under ambient conditions. In benzene-d_6, 2 and 4 equiv of pyridine (**py**) react instantaneously with **1·THF$_2$** and **2·THF$_3$** to yield Mg{Si(SiHMe$_2$)$_3$}$_2$py$_2$ (**1·py$_2$**) and Ca{Si(SiHMe$_2$)$_3$}$_2$py$_4$ (**2·py$_4$**). THF is displaced from the magnesium and calcium coordination spheres, as determined by ^{1}H NMR spectra that contained resonances corresponding to THF dissolved in benzene-d_6. However, an intractable brown oil is obtained upon evaporation of a benzene solution of Mg{Si(SiHMe$_2$)$_3$}$_2$py$_2$ and the displaced THF, and no isolable material is accessible from that reaction. Fortunately, a 1:2 mixture of MgBr$_2$ and pyridine, stirred for 24 h in pentane, gives a suspension that reacts with 2 equiv of KSi(SiHMe$_2$)$_3$ at −30 °C. Careful filtration followed by crystallization at −30 °C provides **1·py$_2$** in 66% yield (Scheme 2).

Reaction either of **2·THF$_3$** and 4 equiv of pyridine in benzene or of pyridine and CaI$_2$ in pentane followed by addition of 2 equiv of KSi(SiHMe$_2$)$_3$ at room temperature produces Ca{Si(SiHMe$_2$)$_3$}$_2$py$_4$ (**2·py$_4$**). Both main-group-metal bis poly(hydrosilyl) pyridine complexes are yellow, highly pyrophoric solids. The SiMe$_2$ signals in the ^{1}H NMR spectra for **1·py$_2$** and **2·py$_4$** were shifted upfield relative to the chemical shifts of the THF analogues, whereas the SiH resonances were shifted downfield. The resonances in the ^{29}Si NMR spectra were comparable for **1·THF$_2$** and **1·py$_2$** with a small shift of ca. 1 ppm in each silicon value. Similarly, the SiHMe$_2$ resonances in **2·THF$_3$** and **2·py$_4$** were nearly equivalent; however, the internal silicon resonance in **2·py$_4$** shifted ca. 5 ppm upfield in comparison to the internal silicon resonance in **2·THF$_3$**. A cross peak in the ^{1}H−^{15}N NMR spectrum of **2·py$_4$** appeared at −80 ppm, which is upfield of the pyridine chemical shift (−68 ppm vs nitromethane). Compound **1·py$_2$** did not show a cross peak in the ^{1}H−^{15}N HMBC experiment. In addition, the IR spectra for **1·py$_2$** and **2·py$_4$** contained bands at 2067 and 2100 cm^{-1}, respectively, assigned to ν_{SiH} that were shifted higher in energy in comparison to **1·THF$_2$** and **2·THF$_3$**.

Crystallization from pentane at −30 °C gives X-ray-quality yellow, needlelike crystals of the bis{poly(hydrosilyl)}calcium tetrakis(pyridine) adduct. The **2·py$_4$** molecule (Figure 3) has a pseudo-octahedral geometry with the silyl ligands disposed trans (∠Si1−Ca1−Si5, 177.86(7)°) and the four pyridine ligands occupying the equatorial sites. The Ca−Si distances of 3.125(3) and 3.147(3) Å are inequivalent; however, the Ca1−N distances (mean Ca−N distance, 2.520 ± 0.008 Å) are equivalent within 3σ error. The Ca−Si distances are slightly longer than the corresponding distances in the five-coordinate Ca{Si(SiMe$_3$)$_3$}$_2$THF$_3$ (3.0421(9) and 3.0861(9) Å),[8b] which is likely related to the difference in coordination number. The Ca−Si distances are slightly shorter than the corresponding distances in the six-coordinate Ca{SiPh$_3$}$_2$THF$_4$ (3.1503(8) Å).[7b] The H atoms belonging to the β-Si atoms were located objectively on the difference Fourier map and were refined isotropically. The Si−H groups point away from the calcium center; this in combination with the IR spectroscopic data rules out secondary interactions in the solid state. The structural features of the silyl ligands in **3·py$_4$** are similar to those groups in KSi(SiHMe$_2$)$_3$ and **3·THF$_3$**, in that the ∠Ca−Si−Si values are larger than those of ∠Si−Si−Si. In addition, the equatorial pyridine rings form a pinwheel-like structure with systematically increasing torsion angles over the four ligands, defined with respect to one of the silyl ligands, giving overall C_1 symmetry in the solid state. The chiral molecule resulting from the pinwheel rotated pyridine groups is related to the enantiomorphic structure through a crystallographic inversion center.

In addition, DMAP reacts with **1·THF$_2$** or **2·THF$_3$** in toluene or benzene to give Mg{Si(SiHMe$_2$)$_3$}$_2$DMAP$_2$ (**1·DMAP$_2$**; eq 4) and Ca{Si(SiHMe$_2$)$_3$}$_2$DMAP$_4$ (**2·DMAP$_4$**; eq 5) in 27%

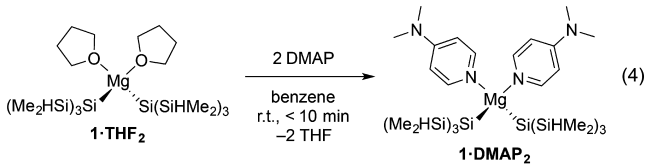

(4)

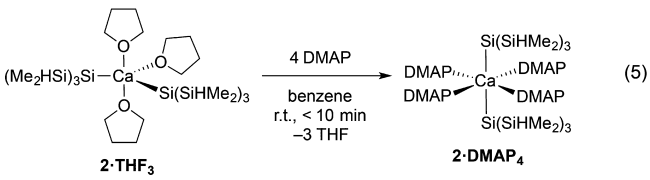

(5)

and 67% isolated yields, respectively. The ^{1}H NMR resonances assigned to the SiHMe$_2$ groups in **1·DMAP$_2$** and **2·DMAP$_4$** were shifted downfield in comparison to the THF and pyridine adducts. The IR band assigned to the Si−H stretching mode for **1·DMAP$_2$** (ν_{SiH} 2083 cm^{-1}) was the highest energy band of the magnesium compounds, while ν_{SiH} for **2·DMAP$_4$** (2036 cm^{-1}) was the lowest energy band of the calcium compounds. A crystallographic study of **2·DMAP$_4$** supports the same octahedral geometry and trans orientation of silyl ligands as in **2·py$_4$**, but the quality of the crystal limits any additional analysis.

Although higher quality crystals are obtained for pyridine and DMAP adducts than for the THF adducts for bis(silyl)calcium species, the pyridine adducts are more thermally labile. Compounds **1·py$_2$** and **2·py$_4$** decompose to intractable brown oils in the solid state at room temperature within 12 h, and thermolysis of **1·py$_2$** or **2·py$_4$** at 60 °C in benzene-d_6 affords Si(SiHMe$_2$)$_4$ as the only observable species in the ^{1}H NMR spectrum after 1 h. The DMAP adducts are more persistent in solution and decompose only slightly faster in comparison to **1·THF$_2$** and **2·THF$_3$**.

The bidentate 2,2′-bipyridine (bipy) ligand further decreases the robustness of the bis{poly(hydrosilyl)}magnesium and -calcium compounds. For example, the reaction of 2 equiv of bipy with **1·THF$_2$** or **2·THF$_3$** in THF-d_8 results in instantaneous formation of a deep red solution. The ^{1}H NMR spectrum of the reaction mixture revealed resonances assigned to Si(SiHMe$_2$)$_4$ and uncoordinated THF in addition to one broad resonance in the aryl region. The reaction mixture is homogeneous, and when the temperature was lowered to 230

DOI: 10.1021/acs.organomet.7b00383
Organometallics XXXX, XXX, XXX−XXX

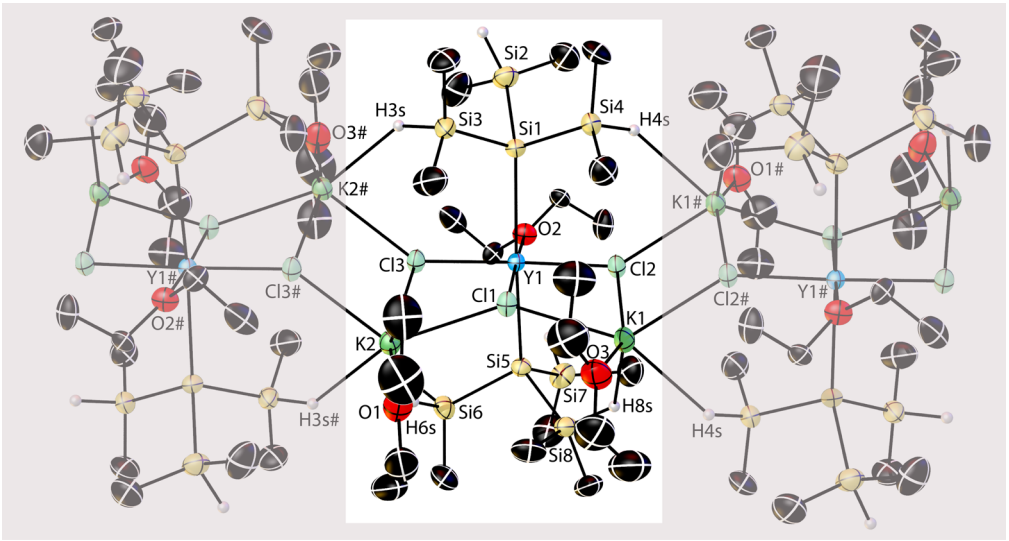

Figure 4. Rendered thermal ellipsoid plot of $K_2Y\{Si(SiHMe_2)_3\}_2Cl_3(OEt_2)_3$ (**4**). The highlighted area illustrates a single repeat unit of the polymeric structure. H atoms bonded to Si centers were objectively located in the Fourier difference map; all other H atoms were placed at idealized locations and refined with isotropic displacement coefficients relative to neighboring atoms. Selected distances (Å): Y1−Si1, 3.039(1); Y1−Si5, 3.030(1); Y1−Cl1, 2.6097(9); Y1−Cl2, 2.6211(9); Y1−Cl3, 2.6240(9); Y1−O2, 2.340(2).

K, the broad aryl resonance resolved into four broad peaks. On the basis of this data, we tentatively assign the metal-containing species as $Ca(bipy)_n$ or $Mg(bipy)_n$ complexes.

A Tris(dimethylsilyl)silyl Yttrium Species. The reaction of anhydrous YCl_3 and 3 equiv of $KSi(SiHMe_2)_3$ in diethyl ether at −78 °C for 8 h yields a diamagnetic compound with the formula $K_2Y\{Si(SiHMe_2)_3\}_2Cl_3(OEt_2)_3$ (**4**). This compound is characterized primarily by X-ray diffraction analysis because it decomposes rapidly at room temperature in solution or in the solid state to several unidentified silyl-containing species. A crystal for diffraction studies was quickly mounted on the diffractometer under a cooled stream of N_2. The crystallographic analysis revealed a six-coordinate yttrium center bonded to two trans-disposed $Si(SiHMe_2)_3$ groups, three meridional Cl ligands, and one disordered Et_2O ligand (Figure 4). The yttrium, two chlorides, and one potassium form a nearly planar four-edged irregular polygon. The yttrium and one chloride are shared between two of these units, which connect to give a nearly planar rectangle with two potassiums (K1 and K2) and two chlorides (Cl2 and Cl3) as vertices, with the long edges bisected by Y1 and Cl1. These rectangles are the repeat units in a ladderlike polymeric chain, which alternate in a syndiotactic fashion with yttrium switching sides from one monomer to the next. Each potassium ion is coordinated by an additional diethyl ether ligand. The $Si(SiHMe_2)_3$ ligands bonded to yttrium are located on both faces of the ladder polymer, and two SiH groups of each $Si(SiHMe_2)_3$ ligand point toward the two potassium centers. Two SiH groups in one of the $Si(SiHMe_2)_3$ ligands bridge to two K centers within the same YK_2Cl_3 unit, while the SiH groups in the second silyl ligand bridge to K centers in adjacent YK_2Cl_3 units; however, the Y1−Si1 (3.039(1) Å) and Y1−Si5 (3.030(1) Å) distances are very similar. These distances are also similar to those for a tris(cyclopentadienyl)yttrium N-heterocyclic silylene adduct (3.038(2) Å)[32] but longer than those in the monosilyl compounds $Y\{Si(SiMe_3)_3\}I_2THF_3$ (2.979(3) Å) and $Y\{Si(SiMe_3)_2Et\}I_2THF_3$ (2.961(2) Å).[8e]

Compound **4** decomposed at room temperature, but crystals were dissolved in toluene-d_8 and analyzed at 200 K by NMR spectroscopy. The ^1H NMR spectrum contained broad resonances at 4.34 ppm assigned to the SiH and another broad resonance at 0.77 ppm assigned to the $SiMe_2$ group (36 H, $^3J_{HH}$ = 4.0 Hz). A $^1H-^{29}Si$ HMBC experiment in toluene-d_8 at 200 K contained cross peaks from these signals to resonances at δ −9.1 and −141.6 ppm for $Si(SiHMe_2)_3$ and $Si(SiHMe_2)_3$, respectively, which are shifted downfield in comparison to $KSi(SiHMe_2)_3$. Unfortunately, the short lifetime of compound **4** prohibited further characterization and reactivity studies.

Reactions of Magnesium and Calcium Silyl Compounds with Lewis Acids. The structural and spectroscopic differences between alkyl $C(SiHMe_2)_3$ and silyl $Si(SiHMe_2)_3$ compounds are expected to affect their reactivity. The alkyl compounds contain secondary β-Si−H⇀M interactions and react with Lewis acids such as $B(C_6F_5)_3$ and BPh_3 via hydrogen abstraction to give $MC(SiHMe_2)_3\{HB(C_6R_5)_3\}THF_2$ compounds. Even though the ligand count is higher in $M\{Si(SiHMe_2)_3\}_2THF_3$ than in the alkyl analogue, the nonclassical interactions in the latter, combined with steric effects, may protect the Ca−C bond from strong electrophiles. As a result, reactions of $M\{C(SiHMe_2)_3\}_2THF_2$ occur at the peripheral SiH. The longer M−Si bonds and two center-two electron classical Si−H bonding in the silyl compounds might reflect lower β-SiH nucleophilicity, and chemistry might instead occur at the M−Si bond in the silyl compounds.

To test for the nucleophilic site in the silyl species, the magnesium and calcium bis{poly(hydrosilyl)} compounds were combined with the Lewis acids $B(C_6F_5)_3$ and $BPh(C_6F_5)_2$. Reactions of **1·THF$_2$** or **2·THF$_3$** and $BPh(C_6F_5)_2$ result in hydride abstraction, which is clearly supported by a doublet at −18.6 ppm ($^1J_{BH}$ = 69 Hz) in the ^{11}B NMR spectra. A well-resolved ^1H NMR spectrum (in benzene-d_6) is obtained for the isolated reaction product from **2·THF$_3$** and $BPh(C_6F_5)_2$ that contains the typical doublet and septet pattern for a $SiHMe_2$. Elemental analysis of the product is consistent with the formulation $CaSi(SiHMe_2)_3\{HBPh(C_6F_5)_2\}$. However, the ^{29}Si NMR chemical shift of the $Si(SiHMe_2)_3$ is −117 ppm, which is significantly downfield from the starting material (−172 ppm). Interestingly, $Si(SiHMe_2)_4$ is obtained from thermolysis of this

DOI: 10.1021/acs.organomet.7b00383
Organometallics XXXX, XXX, XXX−XXX

material, which is also consistent with the formulation of $CaSi(SiHMe_2)_3\{HBPh(C_6F_5)_2\}$.

The reaction of **1·THF$_2$** and $BPh(C_6F_5)_2$ gives spectra similar to those for the calcium congener, although the product is poorly soluble in benzene and requires additional THF for spectroscopic analysis. A downfield ^{29}Si NMR signal at −109 ppm was assigned to $-Si(SiHMe_2)_3$, and this material also yields $Si(SiHMe_2)_4$ upon thermolysis. In contrast, the calcium and magnesium bis(silyl) DMAP adducts react with $PhB(C_6F_5)_2$ to give mixtures. The complicated ^{1}H NMR spectra from reactions performed in benzene-d_6 contained resonances assigned to starting material, DMAP-$BPh(C_6F_5)_2$, and the organosilane products $HSi(SiHMe_2)_3$ and $Si(SiHMe_2)_4$.

A 2 equiv amount of the stronger Lewis acid $B(C_6F_5)_3$ reacts with **1·THF$_2$** or **2·THF$_3$** to cleanly afford $M\{HB(C_6F_5)_3\}_2THF_2$ (M = Mg, Ca),[15b] while 1 equiv of $B(C_6F_5)_3$ reacts with **1·THF$_2$** or **2·THF$_3$** to give a mixture of $M\{HB(C_6F_5)_3\}_2THF_2$, a number of unidentified organosilanes, and ring-opened THF. The byproduct of these hydride abstraction reactions would be $Me_2Si{=}Si(SiHMe_2)_2$, which is expected to be highly labile toward cycloaddition chemistry or oligomerization. However, some evidence for this species is provided by reactions in the presence of the trapping reagent bis(trimethylsilyl)acetylene. Reaction of **2·THF$_3$**, 2 equiv of bis(trimethylsilyl)acetylene, and 2 equiv of $B(C_6F_5)_3$ in benzene afforded a yellow oil containing a mixture of silanes with the major product assigned as 1,2-disilacyclobutene (eq 6).

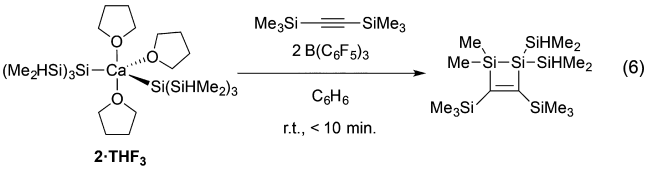

(6)

The ^{1}H NMR spectrum displayed a septet at 3.99 ppm assigned to SiH and a doublet at 0.31 ppm assigned to SiMe within the $SiHMe_2$ groups. Two additional singlets appeared at 0.41 ppm, assigned to $SiMe_2$, and 0.16 ppm, assigned to $SiMe_3$. These peaks were determined to be within the same species rather than from different silanes on the basis of NOESY NMR correlations. We observe the C=C resonances in the ^{13}C NMR spectrum at 197.25 and 195.16 ppm. The ^{29}Si NMR spectrum contained a singlet at −19.6 ppm for $SiMe_3$ and a doublet at −26.2 ppm (^1J = 164 Hz) for $SiHMe_2$. The internal Si peaks were assigned at −135.0 ppm for $Si(SiHMe_2)_2$ and −146.6 ppm for $SiMe_2$. The IR spectrum showed one stretching frequency at 2091 cm^{-1} assigned to ν_{SiH}. Other attempts to trap the disilene and characterize the other silicon-containing products were not fruitful.

Reaction of 3·THF$_3$ and TlTo^M. The reaction of **3·THF$_3$** and $TlTo^M$ (To^M = tris(4,4-dimethyl-2-oxazolinyl)-phenylborate) in benzene at room temperature for 1 day produces $To^M{}_2Yb$ (**5**) (eq 7). Compound **5** is obtained

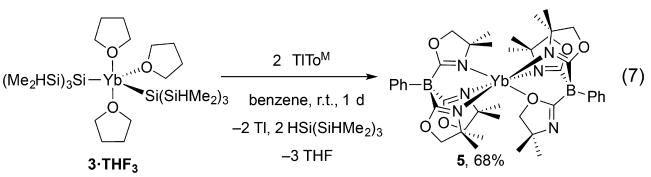

(7)

regardless of the reaction stoichiometry, and its formation rather than heteroleptic $To^MYb\{Si(SiHMe_2)_3\}$ is consistent with the observed lability of $Si(SiHMe_2)_3$ groups.

The ^{1}H NMR spectrum of **5**, acquired in benzene-d_6 at room temperature, contained singlet resonances at 1.14 and 3.40 ppm (36 and 12 H, respectively) assigned to the oxazolinyl methyl and methylene groups. The ^{11}B NMR spectrum contained one resonance at −17.9 ppm, which is shifted upfield from the $TlTo^M$ starting material.[33] Both ^{1}H and ^{11}B NMR spectra are consistent with a structure containing equivalent To^M ligands with oxazoline groups within each To^M ligand related by C_{3v} symmetry.

While a single-crystal X-ray diffraction study shows that the composition of compound **5** is consistent with the formulation on the basis of the above spectroscopy and combustion analysis, the diffraction results reveal a remarkable distinction between the solid-state and solution-phase structures. Compound **5** crystallizes with a six-coordinated ytterbium bonded to six oxazolines; however, the oxazolines are not equivalent in their coordination modes, in that O1 of one oxazoline is coordinated to Yb1, while the remaining five oxazolines are N-coordinated (Figure 5). In addition, the structure reveals considerable bending of the To^M–Yb–To^M coordination, as described by the nonlinear B1–Yb1–B2 angle (147.3(1)°) or the $Cent_{O1,N2,N3}$–Yb1–$Cent_{N4,N5,N6}$ angle (158.6°; Cent is the geometric average of the coordinates of three *fac*-coordinated atoms from each To^M ligand). The distorted geometry is also illustrated by the transoid L–Yb–L angles, which range from 150 to 165°. One of the cisoid angles for two oxazolines is notably obtuse (N3–Yb1–N5, 122.5(1)°). The overall complex lacks symmetry for these reasons. This distortion is in contrast with the linear B–Ln–B angle in divalent, trigonal-prismatic $Tp^*{}_2Ln$ and $\{Tp^{Ph}\}_2Ln$ (Tp^* = $HB(3,5\text{-}N_2C_3HMe_2)_3$, Tp^{Ph} = $HB(3\text{-}N_2C_3H_2Ph)_3$; Ln = Sm, Yb; defined by $R\bar{3}$ or $P\bar{1}$, respectively).[34] Divalent, low-coordinate lanthanide alkyls, such as $Ln\{C(SiMe_3)_3\}_2$ (∠C–Ln–C: Ln = Sm, 143.4(6)°; Ln = Eu, 136.0(2)°; Ln = Yb, 137.0(4)°)[35] and $(C_5Me_5)_2Ln$ (∠Cent–Ln–Cent: Ln = Sm, 140.1°; Ln = Eu, 140.3°),[36] form bent structures, while bulky disilazides $Ln\{N(Si^iPr_3)_2\}_2$ are closer to linear (∠N–Ln–N: Ln = Sm, 175.5(2)°; Ln = Er, 167.8(2)°; Ln = Yb, 166.0(1)°).[37]

In **5**, the O-coordinated oxazoline is contained in the plane of a wedge defined by B1, Yb1, and B2, with oxazoline donors from the second To^M ligand on either side. Likely, interligand steric interactions, exacerbated by the bending of the To^M–Yb–To^M coordination, do not allow the bulkier nitrogen side of this oxazoline to coordinate to the ytterbium center. The Yb1–O1 distance (2.453(3) Å) in **5** is longer than the corresponding distances from THF coordination in **3·THF$_3$** (Yb1–O1, 2.389(4); Yb1–O2, 2.368(4); Yb1–O3, 2.392(4) Å), although it is shorter than all the Yb–N distances. The electron density from the poorer oxygen donor is apparently more stabilizing than noncoordination to give the isomeric, five-coordinate $\{\kappa^2\text{-}To^M\}\{\kappa^3\text{-}To^M\}Yb$. O coordination for an oxazoline is unusual and has previously only been structurally characterized to lithium in a heterobimetallic complex of To^M with iridium.[38] Compound **5** is also the first crystallographically characterized six-coordinate divalent metal compound containing two To^M ligands; instead, four-coordinate $\{\kappa^2\text{-}To^M\}_2M$ (M = Mg, Co, Zn) were previously isolated.[39]

An IR spectrum (KBr pellet) revealed a strong band at 1572 cm^{-1} in the region assigned to C=N stretching modes. In addition, a weak peak at 1650 cm^{-1} was also observed, and we

DOI: 10.1021/acs.organomet.7b00383
Organometallics XXXX, XXX, XXX–XXX

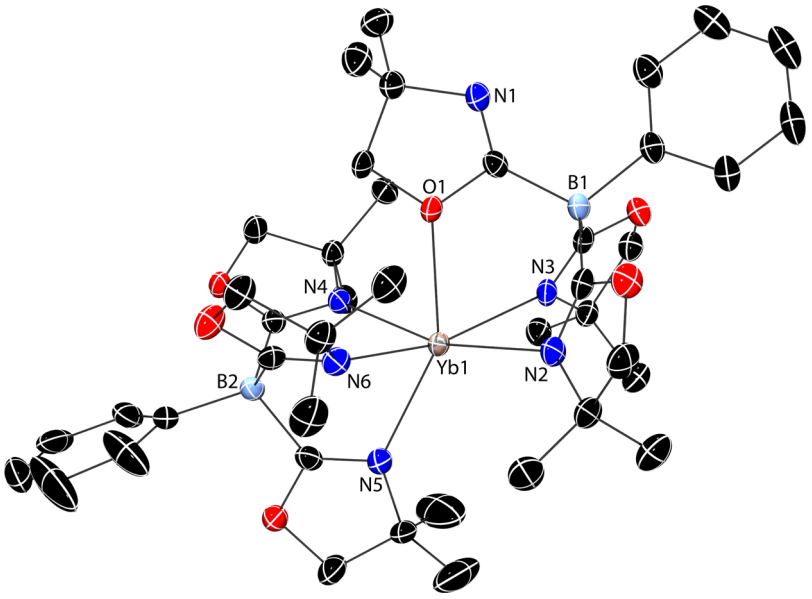

Figure 5. Rendered thermal ellipsoid plot of $To^{M}_{2}Yb$ (**5**). Ellipsoids are plotted at 35% probability. H atoms are excluded from the representation for clarity. Significant distances (Å): Yb1−O1, 2.453(3); Yb1−N2, 2.501(4); Yb1−N3, 2.497(4); Yb1−N4, 2.554(3); Yb1−N5, 2.440(4); Yb1−N6, 2.577(4). Significant angles (deg): O1−Yb1−N2, 85.6(1); N2−Yb1−N6, 94.0(1); N6−Yb1−N5, 78.1(1); N5−Yb1−N4, 77.9(1); N4−Yb1−N3, 97.8(1); O1−Yb1−N3, 99.2(1); B1−Yb1−B2, 147.3(1).

assigned this signal to the $\nu_{C=N}$ of the O-coordinated oxazoline.

CONCLUSION

Highly air and moisture sensitive bis{poly(hydrosilyl)}-magnesium, -calcium, -ytterbium, and -yttrium compounds containing β-SiH moieties have been synthesized. The β-SiH groups are capable of forming K←H−Si bridging structures in polymeric $KSi(SiHMe_2)_3$ and in $[(OEt_2)_2K_2YSi(SiHMe_2)_3)_2Cl_3(OEt_2)]_n$, as was previously observed for the alkyl congener in the structurally distinct dimer $[\{TMEDA\}KC(SiHMe_2)_3]_2$. However, in contrast to related β-SiH-containing bis(alkyl)calcium and -ytterbium compounds, the spectroscopic and structure features of the bis(silyl) compounds rule out side-on secondary interactions involving the central metal. Instead, the bis{poly(hydrosilyl)} compounds bond to divalent metals through classical two center-two electron bonding modes based on the one-bond silicon−hydrogen coupling constants ($^1J_{SiH}$) and the infrared stretching frequencies (ν_{SiH}). In addition, the thermal decomposition pathway of the magnesium and calcium silyl compounds provides $Si(SiHMe_2)_4$, whereas the alkyl compounds afford $HC(SiHMe_2)_3$ upon extended thermolysis. The presence of β-SiH in these silyl compounds does not appear to provide any additional stabilization to the metal−ligand interaction.

Similar to the case for the alkyl analogues, the silyl compounds undergo β-H abstraction rather than silyl group abstraction. Notably, this selective hydride abstraction occurs for secondary-interaction-free compounds, whereas the alkyl compounds contain rapidly exchanging nonclassical M←H−Si and terminal SiH. The reactions of rare-earth and main-group alkyl compounds ($M-C(SiHMe_2)_3$) and Lewis acids are rationalized to occur at the peripheral β-SiH rather than the central C primarily for steric reasons. While the longer M−Si and Si−Si distances in the poly(hydrosilyl) compounds (in comparison to M−C and C−Si distances in the alkyl) might open the silyl group for interaction with electrophiles, the $E(SiHMe_2)_3$ ligand geometry changes from nearly planar for E = C to pyramidal for E = Si. Perhaps this geometric change also limits the nucleophilicity of the central silicon center toward borane Lewis acids.

Alternatively, the electronic structure of both alkyl and silyl ligands may afford sufficient nucleophilicity to the SiH groups, despite the lack of nonclassical bonding in the silyl compounds. That is, the secondary interactions are not needed to activate β-SiH toward hydride abstraction, and perhaps the SiH groups that are not participating in (and not stabilized by) multicenter interactions are more reactive. While the results show that β-secondary interactions are not required for $M-E(SiHMe_2)_3$ moieties to react with electrophiles at the SiH, we observe that reactions of the silyl compounds with Lewis acids are more sensitive to the nature of the Lewis acid and require the weaker $PhB(C_6F_5)_2$ vs $B(C_6F_5)_3$ for selective displacement of one of the silyl ligands. Both silyls in **2·THF$_3$** are readily displaced in reactions with $B(C_6F_5)_3$. Likewise, both silyl ligands are displaced in reactions with $TlTo^{M}$, and we have not yet observed selective substitution of only a single silyl ligand in **3·THF$_3$**.

EXPERIMENTAL SECTION

General Considerations. All reactions were performed under a dry argon atmosphere using standard Schlenk techniques or under a nitrogen atmosphere in a glovebox, unless otherwise indicated. Benzene, toluene, pentane, diethyl ether, and tetrahydrofuran were dried and deoxygenated using an IT PureSolv system. Benzene-d_6 was heated to reflux over Na/K alloy and vacuum-transferred. $TlTo^{M}$,[40] YbI_2,[41] $PhB(C_6F_5)_2$,[42] and $B(C_6F_5)_3$[43] were synthesized according to literature procedures. KO*t*Bu and CaI_2 were purchased from Sigma-Aldrich; the former was sublimed prior to use and the latter was used as received. ^1H, $^{13}C\{^1H\}$, and ^{11}B NMR spectra were collected on a Bruker AVIII 600 spectrometer. ^{15}N chemical shifts were determined by $^1H-^{15}N$ HMBC experiments on a Bruker AVIII 600 spectrometer with a Bruker Z-gradient inverse TXI $^1H/^{13}C/^{15}N$ 5 mm cryoprobe; ^{15}N chemical shifts were originally referenced to an external liquid NH_3 standard and recalculated to the CH_3NO_2 chemical shift scale by adding −381.9 ppm. ^{29}Si NMR chemical shifts were determined by

DOI: 10.1021/acs.organomet.7b00383
Organometallics XXXX, XXX, XXX−XXX

$^{1}H-^{29}Si$ HMBC or HMQC experiments, and $^{1}J_{SiH}$ values were measured from satellites in the ^{1}H NMR spectra. Elemental analyses were performed using a PerkinElmer 2400 Series II CHN/S instrument. X-ray diffraction data were collected on a Bruker APEX II diffractometer.

KSi(SiHMe$_2$)$_3$. KSi(SiHMe$_2$)$_3$ was previously communicated.[20a] The full experimental details and characterization data are reported here, along with results from a single-crystal X-ray diffraction study (see the Supporting Information). Si(SiHMe$_2$)$_4$ (6.00 g, 0.027 mol)[24] and KO*t*Bu (3.95 g, 0.027 mol) were dissolved in a minimal quantity of benzene (ca. 10 mL). The yellow homogeneous solution was allowed to stand for 0.5 h. Over that time, the product precipitated as a white solid. The product was further precipitated by addition of pentane, and the solvent was decanted. The solid product was washed with pentane (3 × 5 mL). An additional quantity of the product was obtained by concentrating the benzene/pentane supernatant. Recrystallization from toluene at −30 °C gave a white crystalline solid (5.99 g, 0.024 mol, 90.7%). ^{1}H NMR (benzene-d_6, 600 MHz): δ 4.22 (sept, 3 H, $^{3}J_{HH}$ = 4.5 Hz, $^{1}J_{SiH}$ = 152 Hz, Si*H*Me$_2$), 0.56 (d, 18 H, $^{3}J_{HH}$ = 4.5 Hz, SiH*Me*$_2$). $^{13}C\{^{1}H\}$ NMR (benzene-d_6, 150 MHz): δ 2.47 (SiHMe$_2$). ^{29}Si NMR (benzene-d_6, 119.3 MHz): δ −23.8 (*Si*HMe$_2$), −202.3 (*Si*(SiHMe$_2$)$_3$). IR (KBr, cm^{-1}): ν 2959 (s), 2894 (s), 2020 (s, ν_{SiH}), 1419 (m), 1242 (s), 1041 (s), 872 (s), 766 (m), 685 (m), 645 (m). Anal. Calcd for $C_6H_{21}KSi_4$: C, 29.45; H, 8.65. Found: C, 29.20; H, 8.51. Mp: 123−125 °C.

Mg{Si(SiHMe$_2$)$_3$}$_2$THF$_2$ (1·THF$_2$). MgBr$_2$ (0.0380 g, 0.200 mmol) and KSi(SiHMe$_2$)$_3$ (0.100 g, 0.409 mmol) were dissolved in THF (10 mL). This solution was stirred for 24 h and then was filtered. Evaporation of the solvent provided a yellow oil, which was dissolved in pentane and cooled to −30 °C to give a white solid (0.0652 g, 0.112 mmol, 55.1%). ^{1}H NMR (benzene-d_6, 600 MHz): δ 4.58 (sept, 6 H, $^{3}J_{HH}$ = 4.2 Hz, $^{1}J_{SiH}$ = 169 Hz, *SiH*Me$_2$), 3.70 (br, 8 H, α-THF), 1.32 (br, 8 H, β-THF), 0.56 (d, 36 H, $^{3}J_{HH}$ = 4.2 Hz, SiH*Me*$_2$). $^{13}C\{^{1}H\}$ NMR (benzene-d_6, 150 MHz): δ 70.44 (α-THF), 25.53 (β-THF), 0.90 (SiH*Me*$_2$). ^{29}Si NMR (benzene-d_6, 119.3 MHz): δ −27.5 (*Si*HMe$_2$), −182.3 (*Si*(SiHMe$_2$)$_3$). IR (KBr, cm^{-1}): ν 2953 (s), 2896 (s), 2064 (s, ν_{SiH}), 1460 (w), 1424 (w), 1244 (s), 1023 (s), 862 (s), 745 (m), 687 (s), 646 (s), 445 (w). Anal. Calcd for $C_{16}H_{50}MgOSi_8$ (corresponding to the loss of 1 THF during analysis): C, 37.86; H, 9.93. Found C, 37.68; H, 9.62. Mp: 60−63 °C.

Ca{Si(SiHMe$_2$)$_3$}$_2$THF$_3$ (2·THF$_3$). CaI$_2$ (0.150 g, 0.510 mmol) and KSi(SiHMe$_2$)$_3$ (0.250 g, 1.02 mmol) were stirred in THF (15 mL) for 48 h. The volatile materials were removed under reduced pressure, leaving a cream-colored residue. The product was extracted with pentane and recrystallized from a concentrated pentane solution at −30 °C to give a white solid (0.187 g, 0.280 mmol, 63.7%). ^{1}H NMR (benzene-d_6, 400 MHz): δ 4.56 (sept, 6 H, $^{3}J_{HH}$ = 4.0 Hz, $^{1}J_{SiH}$ = 162 Hz, Si*H*Me$_2$), 3.84 (br, 12 H, α-THF), 1.48 (br, 12 H, β-THF), 0.57 (d, 36 H, $^{3}J_{HH}$ = 4.0 Hz, SiH*Me*$_2$). $^{13}C\{^{1}H\}$ NMR (benzene-d_6, 100 MHz): δ 69.78 (α-THF), 25.63 (β-THF), 1.76 (SiH*Me*$_2$). ^{29}Si NMR (benzene-d_6, 119.3 MHz): δ −24.6 (*Si*HMe$_2$), −194.6 (*Si*(SiHMe$_2$)$_3$). IR (KBr, cm^{-1}): ν 2958 (s), 2894 (s), 2045 (s, ν_{SiH}), 1421 (w), 1620 (s), 1032 (s), 859 (s), 681 (w). Anal. Calcd for $C_{20}H_{58}CaO_2Si_8$ (corresponding to the loss of 1 THF during analysis): C, 40.34; H, 9.82. Found: C, 40.28; H, 9.53. Mp: 104−106 °C.

Yb{Si(SiHMe$_2$)$_3$}$_2$THF$_3$ (3·THF$_3$). KSi(SiHMe$_2$)$_3$ (0.573 g, 2.34 mmol) and YbI$_2$ (0.500 g, 1.17 mmol) were stirred in 10 mL of THF at room temperature for 24 h. The resulting reddish orange suspension was evaporated to dryness under reduced pressure and extracted with pentane (3 × 5 mL). The extracts were combined, concentrated, and recrystallized overnight at −40 °C to obtain reddish orange crystals of Yb{Si(SiHMe$_2$)$_3$}$_2$THF$_3$ (0.29 g, 0.36 mmol, 30.9%). ^{1}H NMR (benzene-d_6, 600 MHz): δ 4.63 (m, 6 H, $^{1}J_{SiH}$ = 160 Hz, Si*H*Me$_2$), 3.73 (m, 12 H, OCH$_2$), 1.42 (m, 12 H, CH$_2$), 0.61 (d, 36 H, $^{3}J_{HH}$ = 4.0 Hz, SiMe$_2$). $^{13}C\{^{1}H\}$ NMR (benzene-d_6, 150 MHz): δ 69.23 (OCH$_2$CH$_2$), 25.68 (OCH$_2$CH$_2$), 1.85 (SiMe$_2$). $^{29}Si\{^{1}H\}$ NMR (benzene-d_6, 119 MHz): δ −23.99 (SiHMe$_2$), −168.11 *Si*(SiHMe$_2$). IR (KBr, cm^{-1}): ν 2953 (s), 2891 (s), 2045 (w, ν_{SiH}), 1460 (w), 1243 (s), 1031 (s), 858 (w), 680 (s), 643 (s). Anal. Calcd for $C_{24}H_{66}O_3Si_8Yb$: C, 36.01; H, 8.31. Found: C, 36.83; H, 8.40. Mp: 80−85 °C (dec).

Mg{Si(SiHMe$_2$)$_3$}$_2$py$_2$ (1·py$_2$). Pyridine (27.2 μL, 0.340 mmol) was added to a pentane suspension of MgBr$_2$ (0.0310 g, 0.168 mmol), and the mixture was stirred for 24 h at room temperature. KSi(SiHMe$_2$)$_3$ (0.0820 g, 0.335 mmol) was added at −30 °C. The solution was stirred for 3 h at −30 °C and then filtered. The pentane solution was allowed to stand at −30 °C, and this gave a yellow solid which was isolated by filtration (0.0660 g, 0.111 mmol, 65.9%). ^{1}H NMR (benzene-d_6, 600 MHz): δ 8.62 (br, 4 H, *o*-C$_5$H$_5$N), 6.79 (t, 2 H, *p*-C$_5$H$_5$N), 6.59 (br, 4 H, *m*-C$_5$H$_5$N), 4.66 (sept, 6 H, $^{3}J_{HH}$ = 4.2 Hz, $^{1}J_{SiH}$ = 169 Hz, *SiH*Me$_2$), 0.51 (d, 36 H, $^{3}J_{HH}$ = 4.2 Hz, SiH*Me*$_2$). $^{13}C\{^{1}H\}$ NMR (benzene-d_6, 150 MHz): δ 149.62 (*o*-C$_5$H$_5$N), 139.74 (*p*-C$_5$H$_5$N), 125.45 (*m*-C$_5$H$_5$N), 0.74 (SiH*Me*$_2$). ^{29}Si NMR (benzene-d_6, 119.3 MHz): δ −26.3 (*Si*HMe$_2$), −182.2 (*Si*(SiHMe$_2$)$_3$). IR (KBr, cm^{-1}): ν 2957 (s), 2900 (m), 2067 (s, ν_{SiH}), 1595 (w), 1414 (m), 1250 (s), 1022 (s), 887 (s), 858 (s), 834 (s), 797 (m), 752 (w), 699 (m), 677 (m), 650 (s), 623 (m). Anal. Calcd for $C_{17}H_{47}MgNSi_8$ (corresponding to the loss of 1 py during analysis): C, 39.68; H, 9.21; N, 2.72. Found: C, 40.02; H, 9.65; N, 2.28. Mp: 47−49 °C (dec).

Ca{Si(SiHMe$_2$)$_3$}$_2$py$_4$ (2·py$_4$). A mixture of CaI$_2$ (0.0500 g, 0.170 mmol), pyridine (55.0 μL, 0.680 mmol), and pentane (10 mL) was stirred for 24 h, and then KSi(SiHMe$_2$)$_3$ (0.0830 g, 0.339 mmol) was added. The reaction mixture was stirred for 3 h, filtered, and crystallized from the pentane solution at −30 °C, yielding a yellow solid (0.0760 g, 0.0990 mmol, 58.7%). ^{1}H NMR (benzene-d_6, 400 MHz): δ 8.92 (d, 8 H, $^{3}J_{HH}$ = 4.2 Hz, *o*-C$_5$H$_5$N), 6.87 (t, 4 H, $^{3}J_{HH}$ = 7.2 Hz, *p*-C$_5$H$_5$N), 6.75 (t, 8 H, $^{3}J_{HH}$ = 6.0 Hz, *m*-C$_5$H$_5$N), 4.59 (sept, 6 H, $^{3}J_{HH}$ = 4.1 Hz, $^{1}J_{SiH}$ = 160 Hz, *SiH*Me$_2$), 0.43 (d, 36 H, ^{3}J = 4.1 Hz, Si(SiH*Me*$_2$)$_3$). $^{13}C\{^{1}H\}$ NMR (benzene-d_6, 150 MHz): δ 150.60 (*o*-C$_5$H$_5$N), 138.52 (*p*-C$_5$H$_5$N), 124.85 (*m*-C$_5$H$_5$N), 1.33 (SiH*Me*$_2$). $^{15}N\{^{1}H\}$ NMR (benzene-d_6, 60.6 MHz): δ −79.6. ^{29}Si NMR (benzene-d_6, 119.3 MHz): δ −23.3 (*Si*HMe$_2$), −199.3 (*Si*(SiHMe$_2$)$_3$). IR (KBr, cm^{-1}): ν 2963 (s), 2853 (m), 2100 (s, ν_{SiH}), 1878 (w), 1598 (m), 1440 (s), 1342 (w), 1248 (s), 1216 (w), 1150 (w), 1008 (s), 889 (s), 861 (s), 840 (s), 825 (m), 806 (m), 786 (m), 734 (m). Anal. Calcd for $C_{27}H_{57}CaN_3Si_8$ (corresponding to the loss of 1 pyridine during analysis): C, 47.10; H, 8.34; N, 6.10. Found: C, 46.84; H, 8.07; N, 6.09. Mp: 83−85 °C (dec).

Mg{Si(SiHMe$_2$)$_3$}$_2$DMAP$_2$ (1·DMAP$_2$). Mg{Si(SiHMe$_2$)$_3$}$_2$THF$_2$ (0.0240 g, 0.0414 mmol) and DMAP (0.0100 g, 0.0819 mmol) were stirred in benzene (10 mL) for 1 h. The volatile materials were evaporated under reduced pressure, and the residue was recrystallized from pentane at −30 °C to give a white solid (0.0150 g, 0.0221 mmol, 26.6%). ^{1}H NMR (benzene-d_6, 600 MHz): δ 8.47 (d, 4 H, $^{3}J_{HH}$ = 5.4 Hz, NC$_5$*H*$_4$NMe$_2$), 6.03 (d, 4 H, $^{3}J_{HH}$ = 4.2 Hz, NC$_5$*H*$_4$NMe$_2$), 4.85 (sept, 6 H, $^{3}J_{HH}$ = 4.2 Hz, $^{1}J_{SiH}$ = 167 Hz, Si*H*Me$_2$), 1.98 (s, 12 H, NC$_5$H$_4$N*Me*$_2$), 0.67 (d, 36 H, $^{3}J_{HH}$ = 4.2 Hz, SiH*Me*$_2$). $^{13}C\{^{1}H\}$ NMR (benzene-d_6, 150 MHz): δ 155.03 (*ipso*-NC$_5$H$_4$NMe$_2$), 150.02 (*o*-NC$_5$H$_4$NMe$_2$), 107.19 (*m*-NC$_5$H$_4$NMe$_2$), 38.54 (NC$_5$H$_4$N*Me*$_2$), 1.05 (SiH*Me*$_2$). $^{15}N\{^{1}H\}$ NMR (benzene-d_6, 60.6 MHz): δ −327.3 (NC$_5$H$_4$*N*Me$_2$). ^{29}Si NMR (benzene-d_6, 119.3 MHz): δ −26.8 (*Si*HMe$_2$), −184.3 (*Si*(SiHMe$_2$)$_3$). IR (KBr, cm^{-1}): ν 2945 (s), 2083 (s, ν_{SiH}), 1616 (s), 1536 (s), 1445 (m), 1389 (m), 1231 (s), 1114 (w), 1063 (w), 1003 (s), 951 (w), 881 (m), 854 (m), 810 (s), 760 (w), 675 (w), 637 (m). Anal. Calcd for $C_{19}H_{52}MgN_2Si_8$ (corresponding to the loss of 1 DMAP during analysis): C, 40.92; H, 9.40; N, 5.02. Found: C, 41.18; H, 9.36; N, 4.62. Mp: 92−94 °C (dec).

Ca{Si(SiHMe$_2$)$_3$}$_2$DMAP$_4$ (2·DMAP$_4$). Ca{Si(SiHMe$_2$)$_3$}$_2$THF$_3$ (0.200 g, 0.300 mmol) and DMAP (0.146 g, 1.20 mmol) were stirred in toluene (10 mL) for 1 h. Crystallization from the reaction mixture at −30 °C gave a pale yellow solid (0.189 g, 0.200 mmol, 67.2%). ^{1}H NMR (benzene-d_6, 600 MHz): δ 8.93 (br, 8 H, NC$_5$*H*$_4$NMe$_2$), 6.28 (br, 8 H, NC$_5$*H*$_4$NMe$_2$), 4.94 (sept, 6 H, $^{3}J_{HH}$ = 4.2 Hz, $^{1}J_{SiH}$ = 161 Hz, Si*H*Me$_2$), 2.05 (s, 24 H, NC$_5$H$_4$N*Me*$_2$), 0.69 (d, 36 H, $^{3}J_{HH}$ = 4.2 Hz, SiH*Me*$_2$). $^{13}C\{^{1}H\}$ NMR (benzene-d_6, 150 MHz): δ 155.14 (*ipso*-NC$_5$H$_4$NMe$_2$), 150.99 (*o*-NC$_5$H$_4$NMe$_2$), 106.91 (*m*-NC$_5$H$_4$NMe$_2$), 38.43 (NC$_5$H$_4$N*Me*$_2$), 1.81 (SiH*Me*$_2$). $^{15}N\{^{1}H\}$ NMR (benzene-d_6, 60.6 MHz): δ −321.6 (NC$_5$H$_4$*N*Me$_2$). ^{29}Si NMR (benzene-d_6, 119.3 MHz): δ −22.5 (*Si*HMe$_2$), −201.5 (*Si*(SiHMe$_2$)$_3$). IR (KBr, cm^{-1}): ν

DOI: 10.1021/acs.organomet.7b00383
Organometallics XXXX, XXX, XXX−XXX

2926 (s), 2036 (s, ν_{SiH}), 1614 (s), 1532 (s), 1444 (m), 1384 (m), 1230 (s), 1110 (w), 1065 (w), 1001 (s), 949 (w), 887 (m), 859 (s), 826 (m), 804 (s), 754 (w), 678 (w), 640 (w). Anal. Calcd for $C_{33}H_{72}CaN_6Si_8$ (corresponding to the loss of 1 DMAP during analysis): C, 48.47; H, 8.87; N, 10.28. Found: C, 48.41; H, 8.24; N, 10.46. Mp: 104−106 °C.

$K_2(Et_2O)_2[Y\{Si(SiHMe_2)_3\}_2Cl_3(Et_2O)]$ (4). $KSi(SiHMe_2)_3$ (0.830 g, 3.39 mmol) and YCl_3 (0.22 g, 1.13 mmol) were stirred in 10 mL of ether at −78 °C for 8 h. The resulting pale yellow suspension was filtered and evaporated to dryness under reduced pressure at −78 °C to obtain **4** as an off-white solid. The compound was crystallized at −40 °C to obtain colorless crystals of $(KOEt_2)_2[Y\{Si(SiHMe_2)_3\}_2Cl_3(Et_2O)]$ (0.812 g, 1.06 mmol, 76.6%).

Trapped Disilene $Me_2Si{=}Si(SiHMe_2)_2$. $B(C_6F_5)_3$ (0.0200 g, 0.0391 mmol) and bis(trimethylsilyl)acetylene (0.0066 g, 0.0391 mmol), dissolved in benzene, were added to $Ca(Si(SiHMe_2)_3)_2THF_3$ (0.0130 g, 0.0195 mmol). The resulting solution was allowed to react for 10 min, and then the yellow solution was filtered through a plug of neutral alumina. Solvent was removed under reduced pressure to give a pale yellow oil containing a mixture of silanes, including the trapped disilene as the major product. ^{1}H NMR (benzene-d_6, 600 MHz): δ 3.99 (sept, 2 H, $^3J_{HH}$ = 4.2 Hz, Si*H*Me$_2$), 0.41 (s, 6 H, Si*Me*$_2$), 0.31 (d, 12 H, ^3J = 4.2 Hz, SiH*Me*$_2$) 0.16 (s, 18 H, Si*Me*$_3$). ^{13}C{^{1}H} NMR (benzene-d_6, 150 MHz): δ 197.25 (Me$_3$Si-*C*=C-SiMe$_3$), 195.16 (Me$_3$Si−C=*C*-SiMe$_3$), −0.64 (Si*Me*$_2$), −0.21 (Si*Me*$_3$), −0.08 (Si*Me*$_3$), −1.58 (SiH*Me*$_2$). ^{29}Si NMR (benzene-d_6, 119.3 MHz): δ −19.6 (br s, *Si*Me$_3$), −26.2 (d, $^1J_{SiH}$ = 164 Hz, Si(*Si*HMe$_2$)$_2$), −135.0 (s, *Si*(SiHMe$_2$)$_2$), −146.6 (s, *Si*Me$_2$). IR (benzene-d_6 solution, cm^{-1}): ν 2956 (s), 2927 (m), 2989 (m), 2855 (w), 2091 (s), 1644 (m), 1513 (s), 1464 (s), 1375 (m), 1317 (m), 1275 (m), 1249 (s), 1081 (s), 1052 (m), 970 (s), 884 (s), 858 (s), 835 (s), 793 (s). MS: calcd For $C_{13}H_{38}Si_6$: ($M^+ - CH_3$), 359.14; found, m/z 359.24 ($M^+ - CH_3$).

$To^M{}_2Yb$ (5). $Yb\{Si(SiHMe_2)_3\}_2THF_3$ (0.117 g, 0.017 mmol) and $TlTo^M$ (0.197 g, 0.034 mmol) were stirred in 5 mL of benzene at room temperature for 24 h. The resulting red solution was filtered, evaporated to dryness under reduced pressure, and extracted with toluene (2 × 5 mL). The red extracts were cooled overnight at −40 °C to obtain red crystals of $To^M{}_2Yb$ (0.123 g, 0.011 mmol, 68.0%). ^{1}H NMR (benzene-d_6, 600 MHz): δ 8.35 (d, 4 H, *o*-C$_6$H$_5$), 7.57 (t, 4 H, *m*-C$_6$H$_5$), 7.37 (t, 2 H, *p*-C$_6$H$_5$), 3.40 (br, 12 H, CNCMe$_2$*CH*$_2$O), 1.14 (br, 36 H, CNC*Me*$_2$CH$_2$O). ^{13}C{^{1}H} NMR (benzene-d_6, 150 MHz): δ 135.25 (*o*-C$_6$H$_5$), 127.94 (*m*-C$_6$H$_5$), 126.96 (*p*-C$_6$H$_5$), 78.13 (CNCMe$_2$CH$_2$O), 67.73 (CNCMe$_2$CH$_2$O), 28.47 (CNC*Me*$_2$CH$_2$O). ^{11}B NMR (benzene-d_6, 192 MHz): δ −17.9 (s). IR (KBr, cm^{-1}): ν 2963 (s), 2899 (s), 1650 (w), 1572 s ($\nu_{C=N}$), 1463 (s), 1433 (s), 1387 (w), 1367 (s), 1252 (s), 1194 (s), 1176 (m), 1151 (m), 1085 (w), 995 (s), 973 (s), 896 (s), 837 (s), 796 (m), 745 (m), 702 (s), 668 (w), 636 (m). Anal. Calcd for $C_{42}H_{58}B_2N_6O_6Yb$: C, 53.80; H, 6.24; N, 8.96. Found: C, 53.56; H, 6.18; N, 8.72. Mp: 102 °C (dec).

■ ASSOCIATED CONTENT

Supporting Information

The Supporting Information is available free of charge on the ACS Publications website at DOI: 10.1021/acs.organomet.7b00383.

NMR spectra of compounds **2**, **3**, and **5** (PDF)

Accession Codes

CCDC 1551642−1551646 contain the supplementary crystallographic data for this paper. These data can be obtained free of charge via www.ccdc.cam.ac.uk/data_request/cif, or by emailing data_request@ccdc.cam.ac.uk, or by contacting The Cambridge Crystallographic Data Centre, 12 Union Road, Cambridge CB2 1EZ, UK; fax: +44 1223 336033.

■ AUTHOR INFORMATION

Corresponding Author

*E-mail for A.D.S.: sadow@iastate.edu.

ORCID

Aradhana Pindwal: 0000-0002-4547-1290

Aaron D. Sadow: 0000-0002-9517-1704

Author Contributions

†N.L.L. and A.P. contributed equally to this paper.

Notes

The authors declare no competing financial interest.

■ ACKNOWLEDGMENTS

The authors gratefully thank the National Science Foundation (CHE-1464774) for financial support.

■ REFERENCES

(1) (a) Lickiss, P. D.; Smith, C. M. *Coord. Chem. Rev.* **1995**, *145*, 75−124. (b) Lerner, H.-W. *Coord. Chem. Rev.* **2005**, *249*, 781−798. (c) Marschner, C. *Organometallics* **2006**, *25*, 2110−2125.

(2) (a) Ruhlandt-Senge, K.; Henderson, K. W.; Andrews, P. C. Alkali Metal Organometallics. In *Comprehensive Organometallic Chemistry III*; Crabtree, R. H. D., Mingos, D. M. P., Eds.; Elsevier: Oxford, U.K., 2007; pp 1−65. (b) Hanusa, T. P. Alkaline Earth Organometallics. In *Comprehensive Organometallic Chemistry III*; Crabtree, R. H. D., Mingos, D. M. P., Eds.; Elsevier: Oxford, U.K., 2007; pp 67−152.

(3) Miller, G. J. *Chem. Soc. Rev.* **2006**, *35*, 799−813.

(4) (a) Chen, Y.; Song, H.; Cui, C. *Angew. Chem., Int. Ed.* **2010**, *49*, 8958−8961. (b) Pindwal, A.; Ellern, A.; Sadow, A. D. *Organometallics* **2016**, *35*, 1674−1683.

(5) Pindwal, A.; Patnaik, S.; Everett, W. C.; Ellern, A.; Windus, T. L.; Sadow, A. D. *Angew. Chem., Int. Ed.* **2017**, *56*, 628−631.

(6) Harder, S. *Chem. Rev.* **2010**, *110*, 3852−3876.

(7) (a) Buch, F.; Brettar, J.; Harder, S. *Angew. Chem., Int. Ed.* **2006**, *45*, 2741−2745. (b) Leich, V.; Spaniol, T. P.; Maron, L.; Okuda, J. *Chem. Commun.* **2014**, *50*, 2311−2314. (c) Lampland, N. L.; Pindwal, A.; Neal, S. R.; Schlauderaff, S.; Ellern, A.; Sadow, A. D. *Chem. Sci.* **2015**, *6*, 6901−6907.

(8) (a) Bochkarev, L. N.; Makarov, V. M.; Hrzhanovskaya, Y. N.; Zakharov, L. N.; Fukin, G. K.; Yanovsky, A. I.; Struchkov, Y. T. *J. Organomet. Chem.* **1994**, *467*, C3−C5. (b) Teng, W.; Ruhlandt-Senge, K. *Organometallics* **2004**, *23*, 2694−2700. (c) Farwell, J. D.; Lappert, M. F.; Marschner, C.; Strissel, C.; Tilley, T. D. *J. Organomet. Chem.* **2000**, *603*, 185−188. (d) Gaderbauer, W.; Zirngast, M.; Baumgartner, J.; Marschner, C.; Tilley, T. D. *Organometallics* **2006**, *25*, 2599−2606. (e) Sgro, M. J.; Piers, W. E. *Inorg. Chim. Acta* **2014**, *422*, 243−250. (f) Zitz, R.; Hlina, J.; Gatterer, K.; Marschner, C.; Szilvási, T.; Baumgartner, J. *Inorg. Chem.* **2015**, *54*, 7065−7072.

(9) (a) Claggett, A. R.; Ilsley, W. H.; Anderson, T. J.; Glick, M. D.; Oliver, J. P. *J. Am. Chem. Soc.* **1977**, *99*, 1797−1801. (b) Goebel, D. W.; Hencher, J. L.; Oliver, J. P. *Organometallics* **1983**, *2*, 746−750.

(10) Zitz, R.; Hlina, J.; Meshgi, M. A.; Krenn, H.; Marschner, C.; Szilvási, T.; Baumgartner, J. *Inorg. Chem.* **2017**, *56*, 5328−5341.

(11) (a) Lappert, M. F.; Pearce, R. *J. Chem. Soc., Chem. Commun.* **1973**, 126−126. (b) Bradley, D. C.; Ghotra, J. S.; Hart, F. A. *J. Chem. Soc., Dalton Trans.* **1973**, 1021−1023. (c) Atwood, J. L.; Hunter, W. E.; Rogers, R. D.; Holton, J.; McMeeking, J.; Pearce, R.; Lappert, M. F. *J. Chem. Soc., Chem. Commun.* **1978**, 140−142. (d) Hitchcock, P. B.; Lappert, M. F.; Smith, R. G.; Bartlett, R. A.; Power, P. P. *J. Chem. Soc., Chem. Commun.* **1988**, 1007−1009. (e) Rees, W. S. J.; Just, O.; Schumann, H.; Weimann, R. *Angew. Chem., Int. Ed. Engl.* **1996**, *35*, 419−422. (f) Anwander, R.; Runte, O.; Eppinger, J.; Gerstberger, G.; Herdtweck, E.; Spiegler, M. *J. Chem. Soc., Dalton Trans.* **1998**, 847−858. (g) Schumann, H.; Freckmann, D. M. M.; Dechert, S. *Z. Anorg. Allg. Chem.* **2002**, *628*, 2422−2426. (h) Bambirra, S.; Meetsma, A.; Hessen, B. *Organometallics* **2006**, *25*, 3454−3462. (i) Bambirra, S.; van Leusen, D.; Tazelaar, C. G. J.; Meetsma, A.; Hessen, B. *Organometallics* **2007**, *26*, 1014−1023. (j) Wooles, A. J.; Mills, D. P.; Lewis, W.; Blake, A. J.; Liddle, S. T. *Dalton Trans.* **2010**, *39*, 500−510. (k) Huang, W.; Upton, B. M.; Khan, S. I.; Diaconescu, P. L. *Organometallics* **2013**, *32*, 1379−1386. (l) Crozier, A. R.; Bienfait, A. M.; Maichle-Mossmer, C.;

DOI: 10.1021/acs.organomet.7b00383
Organometallics XXXX, XXX, XXX−XXX

Tornroos, K. W.; Anwander, R. *Chem. Commun.* **2013**, *49*, 87−89. (m) Bienfait, A. M.; Schadle, C.; Maichle-Mossmer, C.; Tornroos, K. W.; Anwander, R. *Dalton Trans.* **2014**, *43*, 17324−17332. (n) Conley, M. P.; Lapadula, G.; Sanders, K.; Gajan, D.; Lesage, A.; del Rosal, I.; Maron, L.; Lukens, W. W.; Copéret, C.; Andersen, R. A. *J. Am. Chem. Soc.* **2016**, *138*, 3831−3843. (o) Eedugurala, N.; Wang, Z.; Yan, K.; Boteju, K. C.; Chaudhary, U.; Kobayashi, T.; Ellern, A.; Slowing, I. I.; Pruski, M.; Sadow, A. D. *Organometallics* **2017**, *36*, 1142−1153.

(12) (a) Miller, R. D.; Michl, J. *Chem. Rev.* **1989**, *89*, 1359−1410. (b) Sekiguchi, A.; Lee, V. Y.; Nanjo, M. *Coord. Chem. Rev.* **2000**, *210*, 11−45.

(13) (a) Aitken, C. T.; Harrod, J. F.; Samuel, E. *J. Am. Chem. Soc.* **1986**, *108*, 4059−4066. (b) Tilley, T. D. *Comments Inorg. Chem.* **1990**, *10*, 37−51. (c) Tilley, T. D. *Acc. Chem. Res.* **1993**, *26*, 22−29.

(14) (a) Radu, N. S.; Tilley, T. D. *J. Am. Chem. Soc.* **1995**, *117*, 5863−5864. (b) Radu, N. S.; Tilley, T. D.; Rheingold, A. L. *J. Organomet. Chem.* **1996**, *516*, 41−49. (c) Radu, N. S.; Hollander, F. J.; Tilley, T. D.; Rheingold, A. L. *Chem. Commun.* **1996**, 2459−2460. (d) Radu, N. S.; Tilley, T. D.; Rheingold, A. L. *J. Am. Chem. Soc.* **1992**, *114*, 8293−8295. (e) Castillo, I.; Tilley, T. D. *Organometallics* **2000**, *19*, 4733−4739. (f) Castillo, I.; Tilley, T. D. *Organometallics* **2001**, *20*, 5598−5605. (g) Castillo, I.; Tilley, T. D. *J. Am. Chem. Soc.* **2001**, *123*, 10526−10534.

(15) (a) Yan, K.; Pawlikowski, A. V.; Ebert, C.; Sadow, A. D. *Chem. Commun.* **2009**, 656−658. (b) Yan, K.; Upton, B. M.; Ellern, A.; Sadow, A. D. *J. Am. Chem. Soc.* **2009**, *131*, 15110−15111. (c) Yan, K.; Schoendorff, G.; Upton, B. M.; Ellern, A.; Windus, T. L.; Sadow, A. D. *Organometallics* **2013**, *32*, 1300−1316.

(16) (a) Herrmann, W. A.; Eppinger, J.; Spiegler, M.; Runte, O.; Anwander, R. *Organometallics* **1997**, *16*, 1813−1815. (b) Gorlitzer, H. W.; Spiegler, M.; Anwander, R. *J. Chem. Soc., Dalton Trans.* **1999**, 4287−4288. (c) Eppinger, J.; Spiegler, M.; Hieringer, W.; Herrmann, W. A.; Anwander, R. *J. Am. Chem. Soc.* **2000**, *122*, 3080−3096. (d) Klimpel, M. G.; Gorlitzer, H. W.; Tafipolsky, M.; Spiegler, M.; Scherer, W.; Anwander, R. *J. Organomet. Chem.* **2002**, *647*, 236−244.

(17) Anwander, R.; Roesky, R. *J. Chem. Soc., Dalton Trans.* **1997**, 137−138.

(18) (a) Yan, K.; Heredia, J. J. D.; Ellern, A.; Gordon, M. S.; Sadow, A. D. *J. Am. Chem. Soc.* **2013**, *135*, 15225−15237. (b) Yan, K.; Pindwal, A.; Ellern, A.; Sadow, A. D. *Dalton Trans.* **2014**, *43*, 8644−8653.

(19) Gilman, H.; Holmes, J. M.; Smith, C. L. *Chem. Ind.* **1965**, *20*, 848−849.

(20) (a) Mukherjee, D.; Lampland, N. L.; Yan, K.; Dunne, J. F.; Ellern, A.; Sadow, A. D. *Chem. Commun.* **2013**, *49*, 4334−4336. (b) Lampland, N. L.; Ellern, A.; Sadow, A. D. *Inorg. Chim. Acta* **2014**, *422*, 134−140.

(21) Marschner, C. *Eur. J. Inorg. Chem.* **1998**, *1998*, 221−226.

(22) Gilman, H.; Smith, C. L. *J. Am. Chem. Soc.* **1964**, *86*, 1454−1454.

(23) Lambert, J. B.; Pflug, J. L.; Denari, J. M. *Organometallics* **1996**, *15*, 615−625.

(24) Kulpinski, P.; Lickiss, P. D.; Stanczyk, W. *Bull. Polym. Acad. Sci., Chem.* **1992**, *40*, 21−24.

(25) Ishikawa, M.; Kumada, M.; Sakurai, H. *J. Organomet. Chem.* **1970**, *23*, 63−69.

(26) Bent, H. A. *Chem. Rev.* **1961**, *61*, 275−311.

(27) Klinkhammer, K. W. *Chem. - Eur. J.* **1997**, *3*, 1418−1431.

(28) Jenkins, D. M.; Teng, W.; Englich, U.; Stone, D.; Ruhlandt-Senge, K. *Organometallics* **2001**, *20*, 4600−4606.

(29) (a) Corradi, M. M.; Frankland, A. D.; Hitchcock, P.; Lappert, M. F.; Lawless, G. A. *Chem. Commun.* **1996**, 2323−2324. (b) Niemeyer, M. *Inorg. Chem.* **2006**, *45*, 9085−9095.

(30) Herzog, U.; Roewer, G. *J. Organomet. Chem.* **1997**, *544*, 217−223.

(31) (a) Allen, L. C. *J. Am. Chem. Soc.* **1989**, *111*, 9003−9014. (b) Jeong, N. C.; Lee, J. S.; Tae, E. L.; Lee, Y. J.; Yoon, K. B. *Angew. Chem., Int. Ed.* **2008**, *47*, 10128−10132.

(32) Cai, X.; Gehrhus, B.; Hitchcock, P. B.; Lappert, M. F. *Can. J. Chem.* **2000**, *78*, 1484−1490.

(33) Ho, H. A.; Dunne, J. F.; Ellern, A.; Sadow, A. D. *Organometallics* **2010**, *29*, 4105−4114.

(34) Hillier, A. C.; Zhang, X. W.; Maunder, G. H.; Liu, S. Y.; Eberspacher, T. A.; Metz, M. V.; McDonald, R.; Domingos, A.; Marques, N.; Day, V. W.; Sella, A.; Takats, J. *Inorg. Chem.* **2001**, *40*, 5106−5116.

(35) (a) Eaborn, C.; Hitchcock, P. B.; Izod, K.; Smith, J. D. *J. Am. Chem. Soc.* **1994**, *116*, 12071−2. (b) Eaborn, C.; Hitchcock, P. B.; Izod, K.; Lu, Z. R.; Smith, J. D. *Organometallics* **1996**, *15*, 4783−4790. (c) Qi, G.; Nitto, Y.; Saiki, A.; Tomohiro, T.; Nakayama, Y.; Yasuda, H. *Tetrahedron* **2003**, *59*, 10409−10418.

(36) (a) Evans, W. J.; Hughes, L. A.; Hanusa, T. P. *J. Am. Chem. Soc.* **1984**, *106*, 4270−4272. (b) Evans, W. J.; Hughes, L. A.; Hanusa, T. P. *Organometallics* **1986**, *5*, 1285−1291.

(37) (a) Chilton, N. F.; Goodwin, C. A. P.; Mills, D. P.; Winpenny, R. E. P. *Chem. Commun.* **2015**, *51*, 101−103. (b) Goodwin, C. A. P.; Chilton, N. F.; Vettese, G. F.; Pineda, E. M.; Crowe, I. F.; Ziller, J. W.; Winpenny, R. E. P.; Evans, W. J.; Mills, D. P. *Inorg. Chem.* **2016**, *55*, 10057−10067.

(38) Pawlikowski, A. V.; Gray, T. S.; Schoendorff, G.; Baird, B.; Ellern, A.; Windus, T. L.; Sadow, A. D. *Inorg. Chim. Acta* **2009**, *362*, 4517−4525.

(39) (a) Reinig, R. R.; Mukherjee, D.; Weinstein, Z. B.; Xie, W.; Albright, T.; Baird, B.; Gray, T. S.; Ellern, A.; Miller, G. J.; Winter, A. H.; Bud'ko, S. L.; Sadow, A. D. *Eur. J. Inorg. Chem.* **2016**, 2486−2494. (b) Dunne, J. F.; Fulton, D. B.; Ellern, A.; Sadow, A. D. *J. Am. Chem. Soc.* **2010**, *132*, 17680−17683. (c) Mukherjee, D.; Ellern, A.; Sadow, A. D. *J. Am. Chem. Soc.* **2012**, *134*, 13018−13026.

(40) Ho, H.-A.; Dunne, J. F.; Ellern, A.; Sadow, A. D. *Organometallics* **2010**, *29*, 4105−4114.

(41) Tilley, T. D.; Boncella, J. M.; Berg, D. J.; Burns, C. J.; Andersen, R. A.; Lawless, G. A.; Edelman, M. A.; Lappert, M. F. *Inorg. Synth.* **1990**, *27*, 146−150.

(42) Sundararaman, A.; Jakle, F. *J. Organomet. Chem.* **2003**, *681*, 134−142.

(43) Massey, A. G.; Park, A. J. *J. Organomet. Chem.* **1964**, *2*, 245−250.

DOI: 10.1021/acs.organomet.7b00383
Organometallics XXXX, XXX, XXX−XXX